INTERNATIONAL ATOMIC ENERGY AGENCY
UNITED NATIONS EDUCATIONAL, SCIENTIFIC AND CULTURAL ORGANIZATION

INTERNATIONAL CENTRE FOR THEORETICAL PHYSICS
34100 TRIESTE (ITALY) - P.O.B. 586 - MIRAMARE - STRADA COSTIERA 11 - TELEPHONE: 2240-1
CABLE: CENTRATOM - TELEX 460392-1

SMR/208 - 26

SPRING COLLEGE IN MATERIALS SCIENCE

ON

"METALLIC MATERIALS"

(11 May - 19 June 1987)

ELECTRONIC STRUCTURE AND PHASE STABILITY
(Part V)

F. GAUTIER
L.M.S.E.S.
Université Louis Pasteur
4, rue Blaise Pascal
67070 Strasbourg Cedex
France

V PHASE STABILITY AND PHASE DIAGRAM CALCULATIONS USING CLUSTER EXPANSIONS

1 Introduction

In the previous chapter, we derived cluster expansions for the total energy E. Our aim, in this chapter, is to use both the results of the electronic theory and of the statistical physics to derive "from the first principles" the ground states of binary (at least) systems and the corresponding phase diagrams {T, c} at finite temperature. The relation between the electronic theory of alloys and the phenomenological models introduced in statistical physics is schematically shown in the Table I. A complete phase diagram calculation requires at equilibrium a self consistent determination of the atomic structures and of the of the chemical order : the cluster expansion and the effective PAIR interactions calculated (using) assumptions on the atomic arrangements (atomic volume $\Omega(c)$, crystallographic phases φ, or models for the description of an amorphous state); they determine, at a given temperature, equilibrium (or metastable) states whose characteristics must be consistent with the initial ones.

The only complete phase diagrams deduced using these lines were derived for simple metals using the pseudo potential method (perturbative); let us mention as an example, the system Ca Mg. For transition metal alloys, it's now possible - using the G.P.S. - (1) to have a complete and systematic description of the ground states (GS) i.e. of the possible G.S. (2) to derive the relevant parameters for "building"

TABLE I

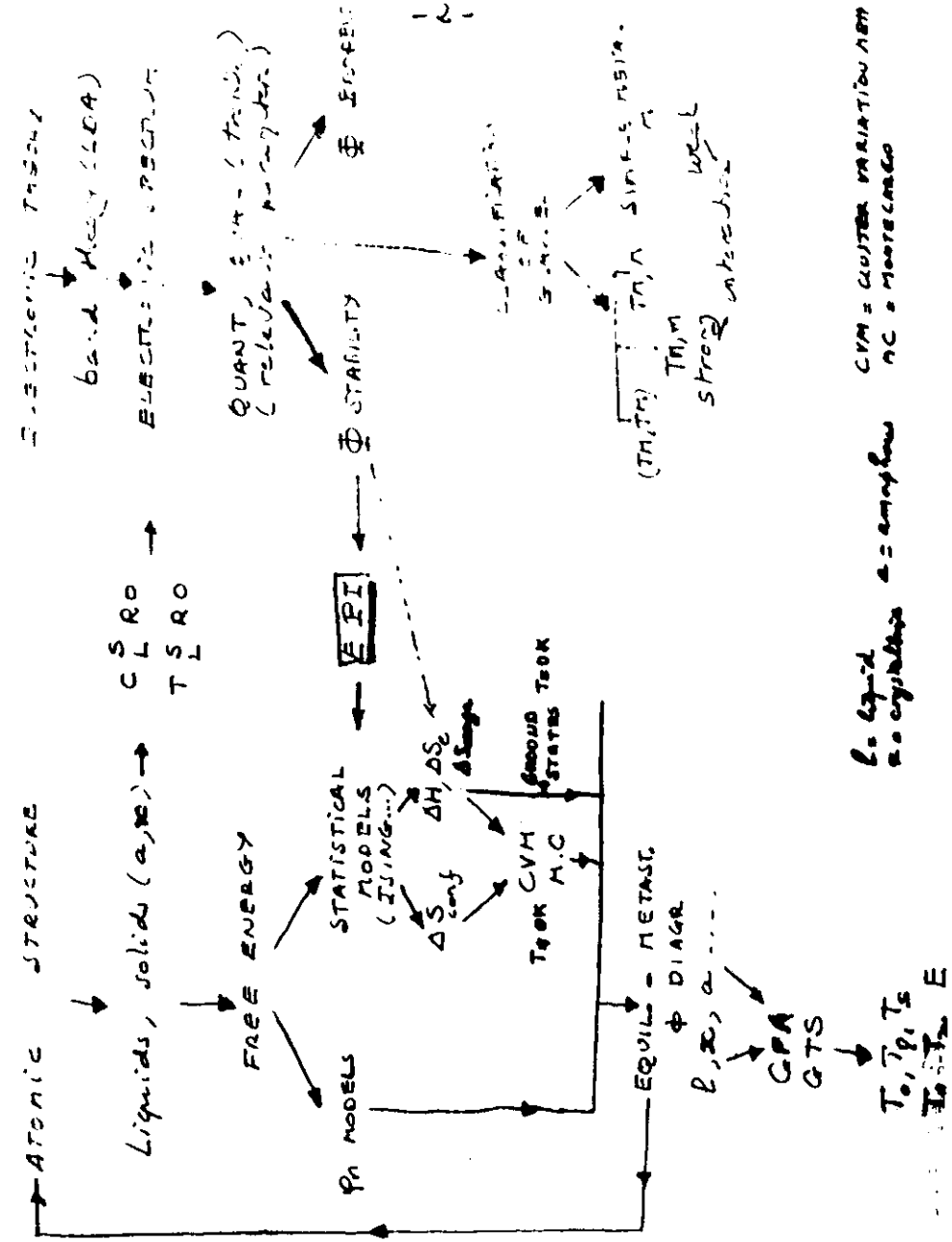

structural maps for homogeneous ordered alloys to derive ground state phase stability at 0K in binary systems (including heterogeneous states). We will discuss here, in a first part, those results (for T=0K) Note that such a systematics has been obtained up to now only in a TB model of "d" bands. Some attempts have been done for sp-d systems so important in metallurgy (semi-empirical TBA) but, up to now there is no "ab initio" comparable systematic study using "1st principles" band structure calculations (KKR GPM for example) in such systems (NiAl etc...)

In the second part of this chapter, we will discuss T≠0K phase stability. After a rapid discussion of the determination of phase diagrams using statistical models (Ising models) we introduce the concept of "prototype phase diagrams" (Dontenwill). We discuss the relation between these phase diagrams and the electronic structure discussed (briefly) the pseudopotential results (Hafner) for normal metals. Then, we relate the SRO parameters to the EPI (or vice-versa) calculated, we show how to use the experimentally determined SRO (in equilibrium) to get informations on the mixing MAI (- see de Novion lectures -). Finally, a rapid discussion of the vibrational, electronic and magnetic excess entropies and of their importance is done; (2) the glass forming ability and stability is discussed in terms of el. structure (if we have time), (3) a first approach of the calculation of the liquid state for transition metal alloys is presented.

-2- GROUND STATE PROPERTIES

2-1 In this section, we first recall some results on the ground state of a 3D Ising model with short ranged interactions (fcc, bcc lattices are chosen as typical examples) such results are known for interactions going (at most) up to the 4th nn in 3D: we showed in the previous chapter that the PI are negligible for n>4 so that those results can be applied to TM alloys. THEY ALLOW TO GET ON A GIVEN LATTICE THE MOST STABLE OS - We apply this method to the determination of structural maps for fcc AB and bcc lattices - Then, we discuss the APB energy in relation with the occurrence of long periods.

We consider for simplicity the Ising model with only pair interactions and we use the notation:

$$E_{conf} = N_a \sum_i v_i p_i$$

where E_{conf} is the part of the energy which depends on the configuration, p_i is the nb of pairs of ith nn type on atom and v_i is the corresponding irreducible pair interaction.

2-2 DETERMINATION OF THE GROUND STATE OF AN ISING MODEL - PRINCIPLE

-1- WE START FROM THE CONFIGURATION ENERGY

$$E = \sum_i V_i P_i \quad (1)$$

V_i = pair interactions between ith neighbours.

P_i = nb of ith pairs

THE GROUND STATE IS DETERMINED BY THE SET

$$\{ P_0 = C, P_1, P_2, \dots \}$$

WHICH MINIMIZES

$$\sum_i V_i P_i$$

THE RANGE OF THE INTERACTIONS MUST BE LIMITED TO SOLVE THIS PROBLEM IN 3d.

UP TO THE n-4^{th} NEIGHBOURS ! (FOR THE fcc LATT

Principle

- DETERMINE GEOMETRICAL INEQUALITIES ON P_i

$$\sum a_{ij}^{(n)} P_j \leq k^{(n)} \qquad n = 1, 2, \dots$$

FROM THE RELATIONS BETWEEN
PAIR - NUMBERS - CONCENTRATION
TRIPLETS- " - "
....

- THEY DEFINE A CONVEX "POLYEDRA (P)" IN THE SPACE $\{P_i\}$: REAL STATES ARE INSIDE
- FOR FIXED V_i, THE LOCUS OF CONSTANT ENERGY IS A PLANE $\perp$ to $(V_1, \dots V_n)$ (eq (1))
- THE ENERGY IS MINIMUM WHEN THE VERTEX OF (P) WHOSE DISTANCE TO THE ORIGIN IS MINIMUM CORRESPONDS TO AN IDENTIFIED STRUCTURE.
- SEVERAL METHODS TO FIND INEQUALITIES (LAND → SINCERE → FINGER)

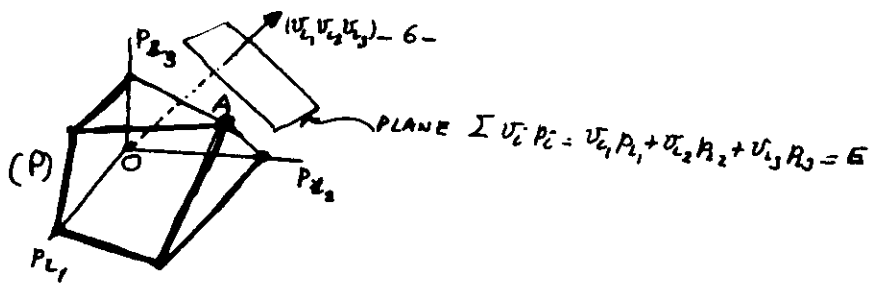

SCHEMATIC
(3 interactions $V_{i_1}, V_{i_2}, V_{i_3}$)
IF THE A VERTEX CORRESPONDS TO AN IDENTIFIED STRUCTURE, IF IT'S THE NEAREST VERTEX FROM 0 THIS STRUCTURE IS THE GROUND STATE

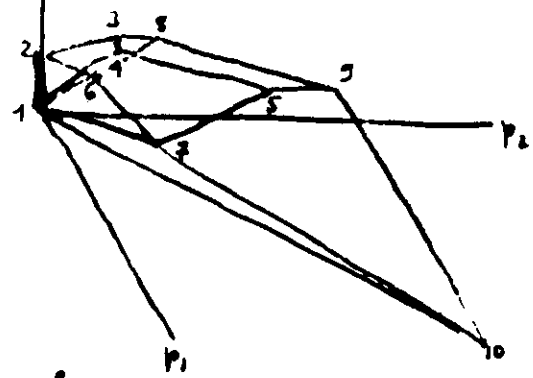

Ex 1 THE CONFIGURATION POLYEDRON hcp $n = 2$

Ex 2 fcc : $V_1, V_2 \neq 0$ $V_n = 0$ $\forall n \geq 2$: THE INEQUALITIES WHICH DETERMINE THE CONFIGURATION POLYEDRON ARE

$A = P_1 \geq 0$ $\quad c \leq 1/4$, $\geq N(4c-1)$ $\quad 1/4 < c < 1/2$

$B = 2P_1 + P_2 \geq 0$ $\quad c < 1/6$ $\quad \geq N(6c-1)$ $\quad 1/6 \leq c \leq 1/3$

$\geq N(12c-3)$ $\quad 1/3 \leq c \leq 1/2$

$C = P_2 \geq 0$ $\quad x \leq 1/2$

$D = P_2 - P_1 \geq -3c$

$F = -P_2 \geq -3c$

fcc $n = 2$

2-2-1 Discussion of the results for simple structures.

For two interactions $V_1, V_2 \neq 0$ ($V_n (n>2) = 0$), we can define on the plane (V_1, V_2) the domains for which the structures are the most stable. The exact results derived by the previous method are a small bit different from those derived in a mean field approximation. Note that :

- (1) Some of the structures observed experimentally are not stabilized by this Ising model and several ones which are predicted are degenerate. For example, in the bcc lattice, only B2 ("CsCl"), B32 ("NaTl") and DO_3 ("Fe_3Al") structures are stabilized whereas the γ fcc Cu structure, needs $V_3 \neq 0$ to be stabilized [and "$MoSi_2$" (CM_6) structure (with A_5B and A_5B_2 are never observed in TM alloys whereas "CuPt" is the only one system for which such structure occur.
- The pb (1) can be solved by considering more and more distant neighbours. (prediction of the stability of Long Periods in the fcc lattice - example of $TiAl_3$: see later)
- The pb (2) can only be understood by an electronic structure calculation of (V_1, V_2) which will determine the domain for which real systems exist. For example, in TM alloys we know that, for fcc lattices, $|V_2| \ll |V_1|$ so that a "CuPt" order is practically impossible ; on the contrary, in substoechiometric compounds $M_{xx} C_{1-x}$ we noted (chapter I) the existence of a large number of "CuPt" O.S (of C vacancy on its sublattice). This is also natural since by moments arguments we showed that in such a case $|V_2| \geq |V_1|$ (see NOVION lectures.)

PREDICTED GROUND STATES IN A 3D ISING MODEL FOR fcc AND bcc LATTICES ($V_3 = 0$, $V_{n>2} \neq 0$)

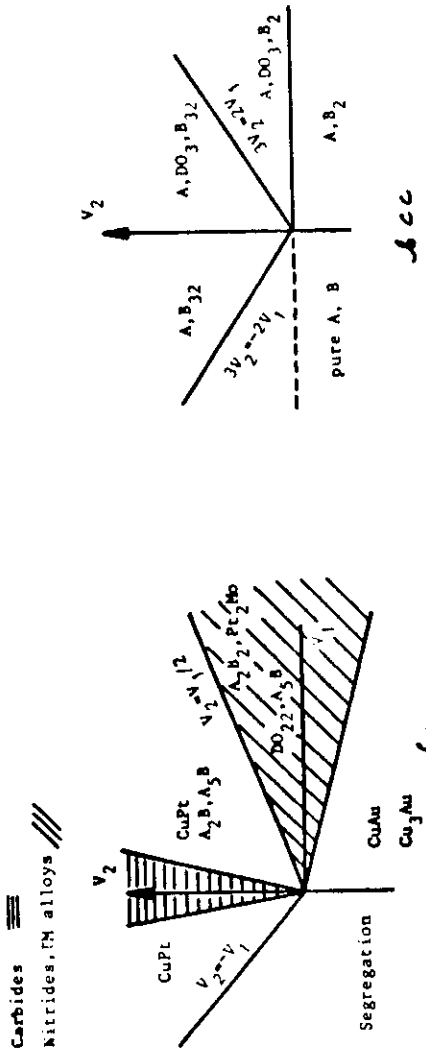

THE SHADED REGIONS SHOW THE "PHYSICAL" REGIONS ; FOR TM AL SYST (V_2) $\ll$ (V_1).

In the following, we will use the KANAMORI KAKEHASHI results for the fcc lattice (up to V_4). An example of the phase stability which is predicted is given below: the relative stability of the DO_{22} and of the $L1_2$ structures (which differ by periodic APB is determined for $V_4 < 0$ only by the sign of the APB energy (see below)

$$\xi = V_2 - 4V_3 + 4V_4.$$

When $\xi > 0$ $L1_2$ is stable, when it's negative it's unstable and DO_{22} is stable. (see below the section on APB) For $V_4 > 0$ this condition is still necessary but it's no more sufficient (see fig p 10).

2.3 GENERALIZED STRUCTURAL MAPS (GSM) FROM THE G.P.M.

(for all the next sections see A Berbier. F Similar Acta Met Overview (1985).)

We consider here only HOMOGENEOUS O.S, FOR GIVEN CONCENTRATION c AND STRUCTURE φ (fcc, hcp, bcc ...)

The PI $V_n^{\varphi}(c, \delta, \bar{N})$ are calculated for TM alloys in the GPM framework. The previous results on the ground state stability are then determining for each value of the set $(\delta, \bar{N})$ THE MOST STABLE O.S on the considered lattice φ and for the concentration c. We can then draw GENERALIZED STRUCTURAL MAPS corresponding to domains in the plane $(\bar{N}, \delta_1)$ (or in the 3D space $(\bar{N}\ \delta_1, \delta_{nd})$) for which a given O.S is stable. We present such maps for any fcc lattice ($c = \frac{1}{4}, \frac{1}{2}$) and for a bcc lattice ($c = \frac{1}{2}$)

We note that: – $L1_2$ and DO_{22} are the only stable structures in the fcc lattice at $c = \frac{1}{4}$

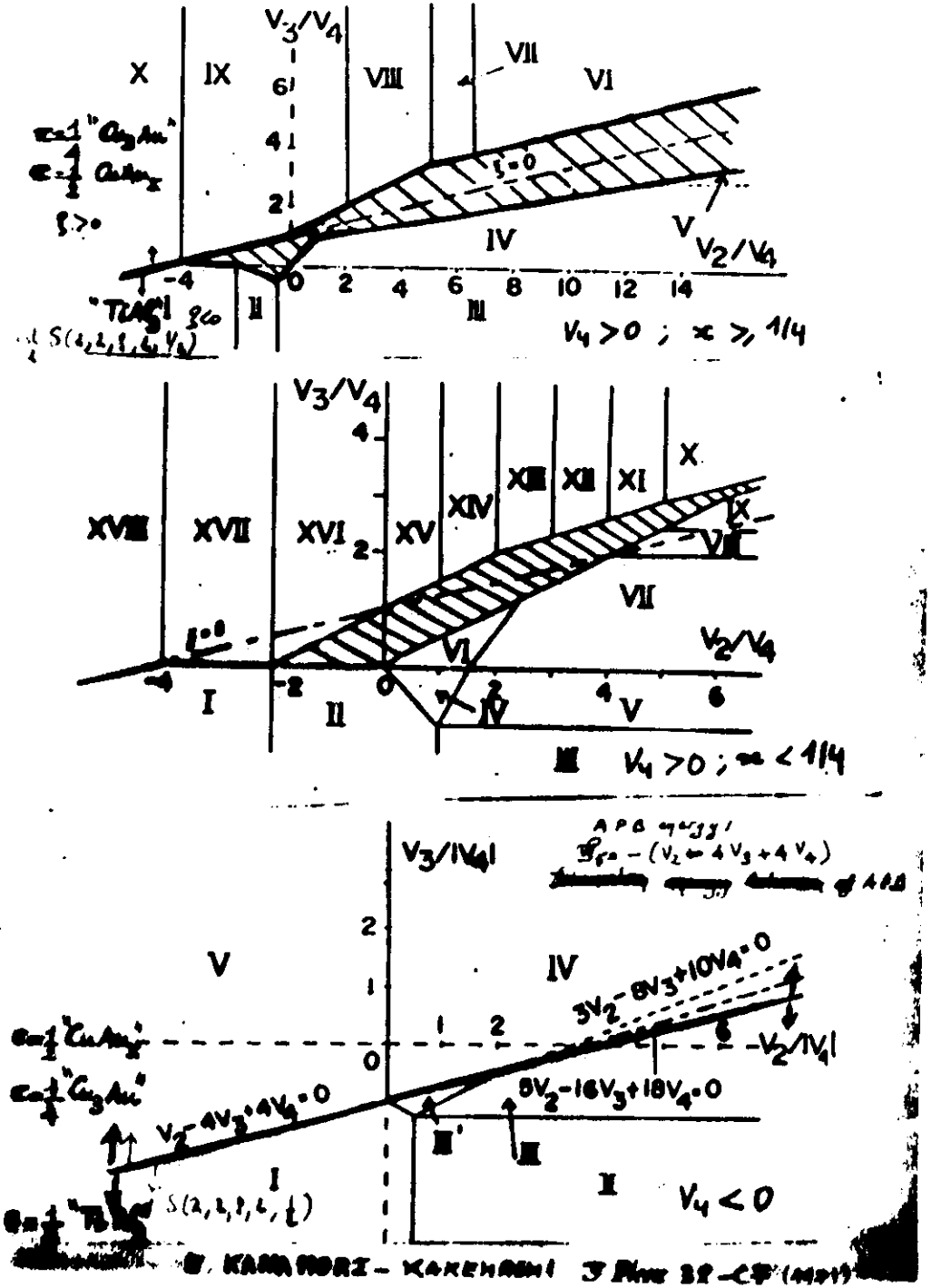

F. KANAMORI – KAKEHASHI J Phys 38 – C7 (1977)

GENERALIZED STRUCTURAL MAPS (G.S.M)

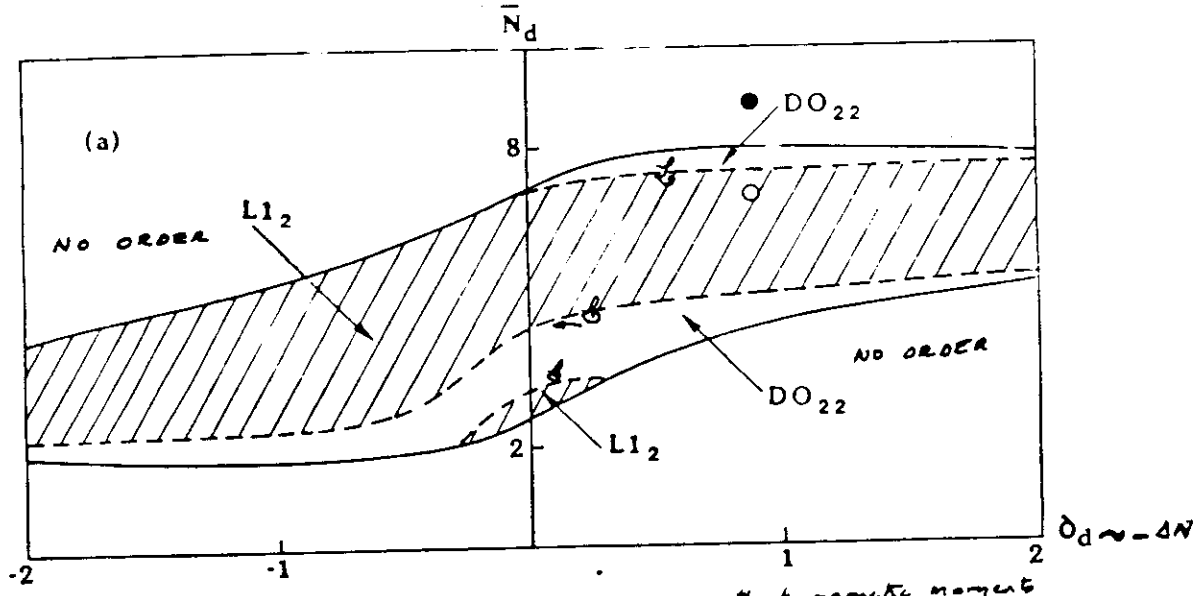

● This corresponds roughly to Ni$_3$Fe (ΔN_{Ni_3Fe} (NMO) without magnetic moments

○ " " " " " STRONG FERROMAGNET Ni$_3$Fe

($V = V_f(\frac{N_A}{2}, \delta_f) + V_\phi(\frac{N_A}{2}, \delta_\phi)$: is a STRONG FERROMAGNET : $V_f \neq 0$, $V_\phi(\frac{N_A}{2}, \delta_\phi) = V$)

from A BIERER & FEANTIER

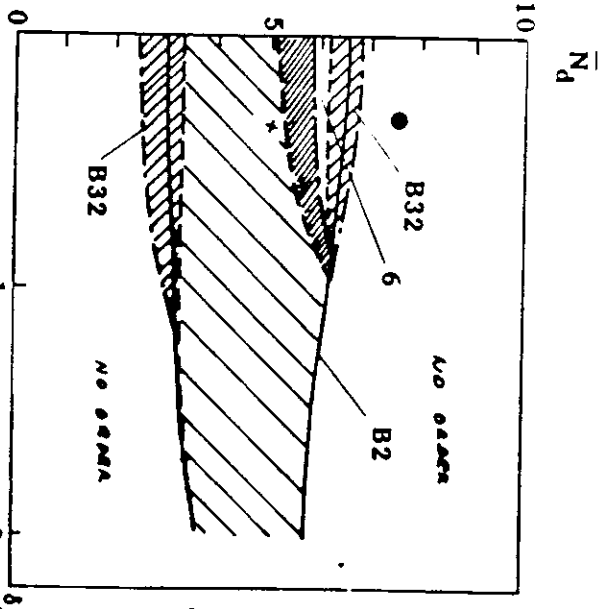

● This corresponds roughly to Fe Co alloys (without any

× " " " " ferromagnetic Fe Co (very

(magnetically ordered moment stabilize the O.S

from A. Bierer & Feantier

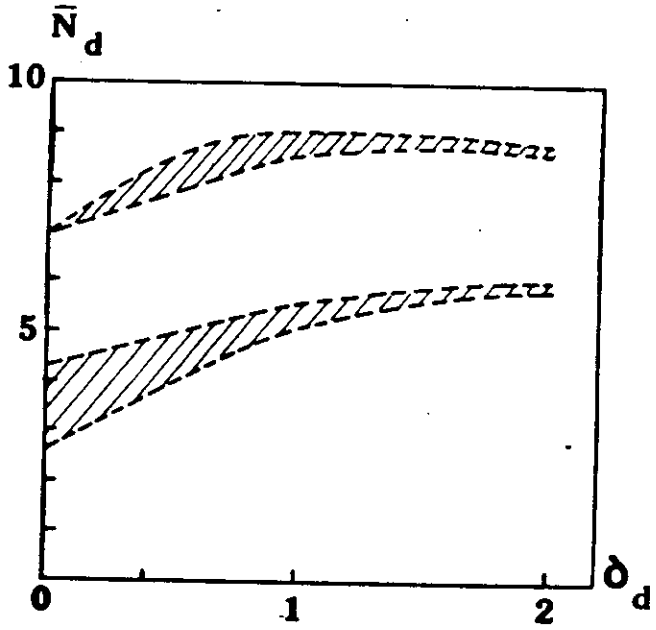

"Pt_8T_i"
(from A. BIEBER AND GAUTIER)

COMPARISON OF THE PREDICTED RANGES OF HOMOGENEOUS ORDERING WITH THE EX " AND FOR A "TYPICAL" VALUE OF δ_d

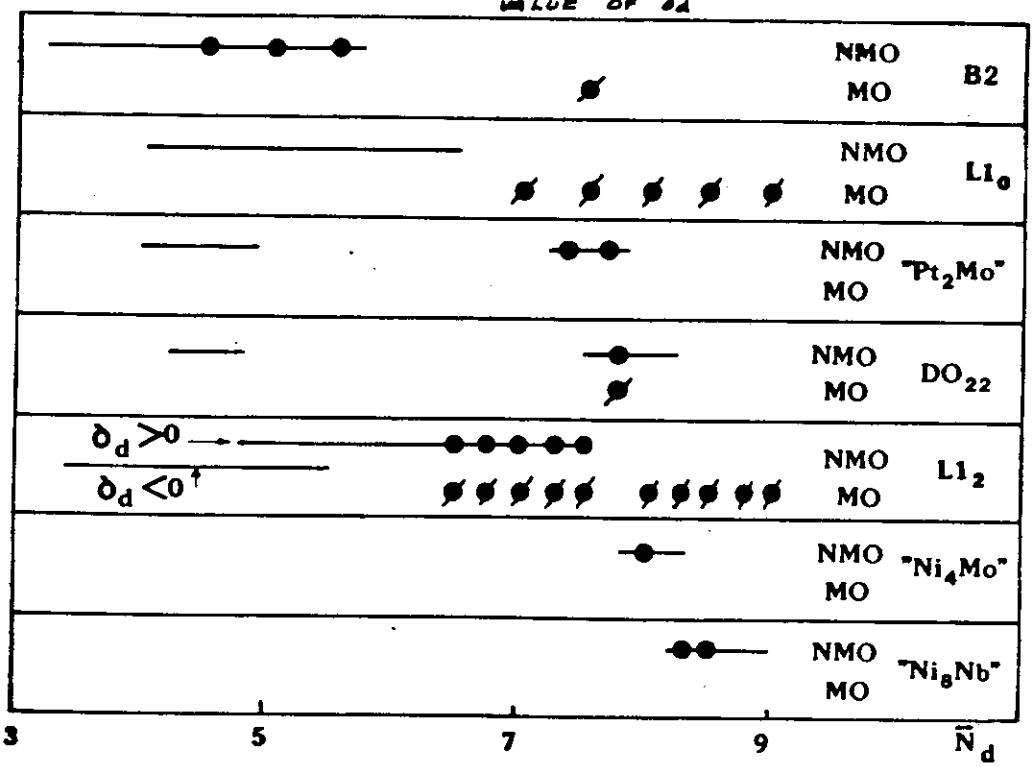

observed { ● non magnetically ordered TM - TM
ø magnetically ordered systems

—— range of band fillings for which non magnetically ordered compounds are predicted

CONCLUSION : OK FOR NMO ; MAGNETISM INDUCES O.S. FOR LARGE $\bar{N}_d$

MAGNETISM AND GROUND STATE PHASE STABILITY.

We showed the importance of magnetism upon phase stability via the G.S.M and the phenomenological structural maps. Magnetic order induces the stabilization of ordered structures which would have otherwise too large values of $\bar{N}$. The mechanism is easy to understand. The previous GSM were built for a given spin direction σ ($\sigma = \uparrow, \downarrow$): $E(N_\sigma, \delta_\sigma)$ is σ independent in a non magnetic system. This is no more true in a ferromagnetic system for which the band fillings and δ_σ are spin dependent:

$$E = E_\uparrow(N_\uparrow, \delta_\uparrow) + E_\downarrow(N_\downarrow, \delta_\downarrow) \quad \text{(ferromagn)}$$

In a strong ferromagnet, one of the bands is filled (e.g. that): $E_\uparrow = 0$; $N_\uparrow^+ = \frac{\bar{N} + \bar{m}}{2}$ (where $\bar{m}$ is the magnetization so that the majority spin band is less filled than in the non magnetically ordered state: eg 0.5 is then stabilized by magnetism (see the G.S.M. and the examples of FeCo and Ni_3Fe alloys. p 11 and 12). A detailed study of these effects have been done at $T = 0K$ and $T \neq 0K$ (Bieber and Gautier to be published JPMM)

$L1_0$ (exp observed)

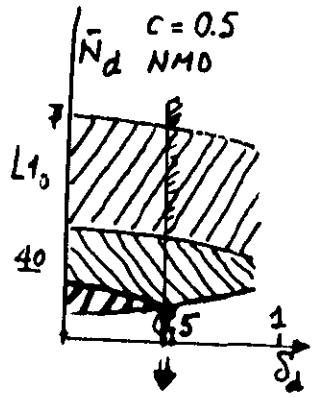

		$\bar{N}_d$	ΔN
Cr Pt	AF	7	-4
Mn Rh	AF	7	-2
Mn Ir	AF	7	-2
Mn Ni	AF	7.5	-3
Mn Pt	AF	7.5	-3
Fe Ni	F	8	-2
Fe Pd	F	8	-2
Fe Pt	F	8	-2
Co Pt	F	7.5	-1
Ni Pt	NMO	9	0

?! (except PtNi)

- ALL THE OBSERVED $L1_0$ STRUCTURES ARE MAGNETIC
- ALL THE MAGNETICALLY ORD. STRUCTURES ARE OUT OF THE PRED RANGE FOR NM.a.s

$L1_2$ (exp observed)

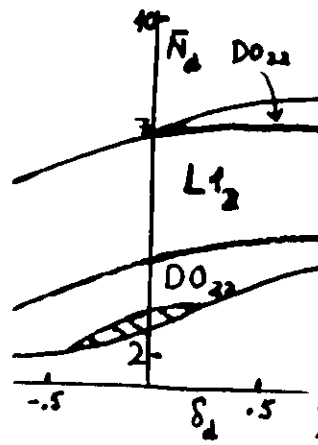

	$\bar{N}_d$	ΔN
Sc Rh	6.5	-6
Sc Pd		
Sc Pt		
Y Pd		
Y Pt		
La Pd		
La Pt		
Ti Co	6.75	-5
Ti Rh		
Ti Ir		
Ti Pt		
Zr Rh		
Zr Ir		
Hf Rh		
Hf Ir		
V Rh	7	
V Ir	7	
Nb Rh	7	
Nb Ir	7	
Ta Rh	7	
Ta Ir	7	-4

A B_3		$\bar{N}_d$	ΔN
Cr Ir	F	7.25	-3
Cr Pt	F	8	-4
Mn Pt	F	7.25	-3
Fe Ni	F	7.5	-2
Fe Pd	F	7.5	-2
Fe Pt	AF	7.5	-2
Co Pt	F	7.75	-1
Rh Mn	AF	6.5	+2
Ir Mn	AF	6.5	+2
Pt Mn	AF	6.25	+3
Pt Fe	F	7.5	+2
Pt Co	F	7.25	+1
Pt Ni	F ? NMO	9	0

NMO

NMO

STRUCTURAL MAP INCLUDING BOTH
fcc and "A15" lattices

THIS MAP MUST BE COMPARED TO THE EXPERIMENTAL ONE
THE DOMAINS FOR WHICH A15 ($\delta N > 0$), $L1_2$ and DO_{22} ARE BEING
FOUND ARE IN THE PREDICTED RANGES.

A_3B
($\delta_{nd}=0$)

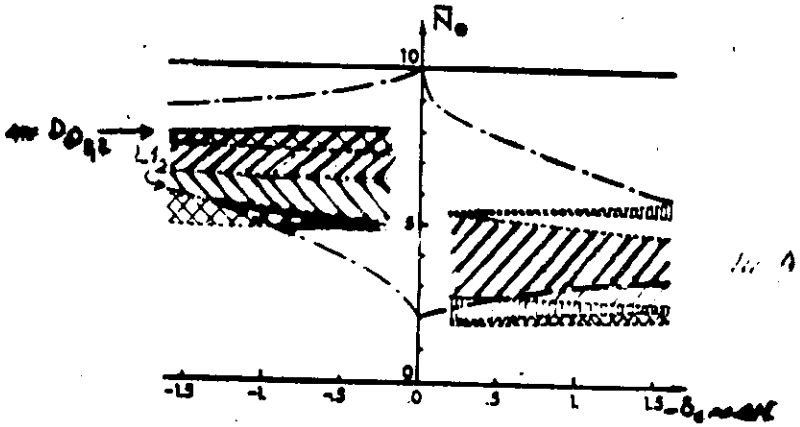

COMPARE WITH THE PHENOMENOLOGICAL MAP
(chapter 4)
from P. TURCHI
(Thesis 1980)

- The separation between the domains of O.S and the others is determined roughly by $V_3 \simeq 0$ (in the fcc lattices) which is only important to determine ΔE_{ord} (this is no more the case for bcc alloys where $|V_2| \sim \frac{1}{2}|V_3|$.
- The G.S.M are symetric in δ_d for $c = .5$, so that the δ_d value is not too much relevant to determine the ranges of band fillings for which a given O.S is the most stable. However, it becomes more and more important to use the 2D map when c becomes smaller and smaller. As an example, we show the range of $\bar{N}_d$ for which several structures are stable for a typical δ_d value (but, caution!)
- In agreement with the phenomenological structural maps:
  - we don't find OS of the "Cu Pt" ($L1_1$) family
  - we find broad regions of stability for DO$_{22}$ and $L1_2$ which are in agreement with experiment and narrow stability regions for DO_{22}, "Pt_3V", Pt_2 Mo type structures
- In bcc lattices, the study is not complete (the results on the Ising model are not available (for $A > 2$) up to now, except for V_1, V_2, V_3 fixed for $c = 0.5$). Nevertheless, the range of the B2 stability is well reproduced ... except for magnetically ordered structures (see below)
- The separation line between $DO_{22} - L1_2$ etc... defining the region for which APB change of sign with band filling $\bar{N}_d$ (well predicted)
- NOTE THAT, for a comparison with experiment, THE EXPT points must be in the regions of stability of the corresp. O.S. in the G.S.M. but, reciprocally, the homogeneous OS can be unstable vs. P...

so that it's possible that no experimental points corresponds to the predicted domain of stability for an O.S

2-A LONG PERIOD APB STRUCTURES AND HIERARCHY OF P.I ON A LATTICE OF [illegible]

We consider only the APB which where defined in chapter I for fcc alloys. Long periods can occur in a simple one dimensional model (neglect of the possible defects in each APB plane) when the axial interactions between two 1st nn mixed planes, ($w_1 > 0$ or $w_1 < 0$) compete with the second nn interactions ($w_2 > 0$) and introduce frustration. Each mixed plane is indexed by its position n and by an index σ ($\sigma = \pm 1$) which characterizes one of the two possible occupations of the lattice by A and B atoms (see fig in 1st chapter). The energy of the crystal for a given configuration $\{\sigma_i\}$ can then be rewritten as :

A_3B

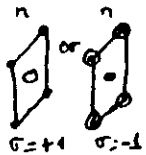

$$E = \sum v_i p_i \Rightarrow E(\{\sigma_n\}) = \sum_n w_1 \sigma_n \sigma_{n+1} + \sum_n w_2 \sigma_n \sigma_{n+2} + \dots$$

We consider here only w_1 and w_2 (w_n $n > 2$ is zero)
The following relations are easily found for the pair energies :

$$\begin{cases} w_1 = (-v_2 + 4v_3 - 4v_4 - \dots + 8v_7 \dots + -) \\ w_2 = (-2v_2 + 8v_3 + \dots - -) \end{cases}$$

- When $w_1 < 0$ ($w_2 = 0$) the ground state is $L1_2$ (+ + + +) : the APB are not stable ; when $w_2 > 0$ ($w_1 = 0$) the ground state is:

$$+ + - - + + - - \quad (DO_{22})$$

for which there are no 2d nn identical mixed planes. There is therefore an exchange of stability when w_2 increases for a given w_1 : the w_1 lowers the energy of the configurations + + + ; the w_2 lowers the energy of + + - - + + - - but there is no way to minimize simultaneously both 1st nn and 2nd nn terms (frustration)

- In the same way, when $w_1 > 0$ ($w_2 = 0$), the ground state is + - + - (DO_{22}) so that increasing $w_2 > 0$ there will be an exchange

of stability between $D0_{22}$ and DO_{23}. The APB energy γ is then defined either from the $L1_2$ ground state (1st case, $w_1 < 0$) or from the DO_{22} state (2d case $w_2 > 0$). These APB have then a formation energy $\gamma = \frac{|w_1|}{2} - w_2$ which decreases from positive values (for small w_2 values) to negative values (for large w_2). They interact when they are 1st nn (with the energy w_2) so that the $L1_2$ ($w_1 < 0$) or the DO_{22} ($w_2 < 0$) becomes unstable for $w_2 > \frac{|w_1|}{2}$ as compared to DO_{23} for which there is the maximum number of APB (consistant with w_2).

Long period structures can then develop near the multiple phase point $w_2 = \frac{|w_1|}{2}$ at $T \neq 0K$ ($\langle 2^n 3 \rangle$ or $\langle 2^n 1 \rangle$ $n = 1, 2 \dots$) in low temperatures and then an entropy stabilization. (see below)

(a) In order to get the simplest long periods we see therefore that it's necessary to take into account LONG RANGED PAIR INTERACTIONS. To get DO_{22}, it's necessary to consider at least PAIR INTERACTIONS BETWEEN THE 8th NN - If we consider only v_n $n \leq 8$, long period APB structures such as observed in NbMo or in Cu Pd can then stabilized at non zero temperatures by entropy effects.

(b) - At zero temperature, it's possible to get such long periods by considering longer ranged pair interactions - For example, if W_n is a convex potential of infinite range, we get in the ground state an infinit number of states as illustrated by the upper figure ("DEVIL STAIRCASE"). Is it physical for TM alloys or sp-d alloys ?

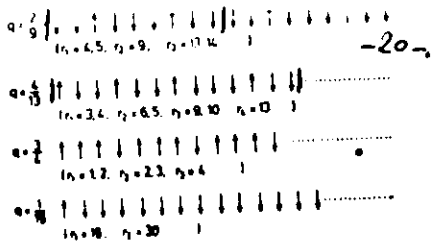

FIG. 1. Typical stable spin configurations with c the ratio of up spins over down spins.

escalier du diable complet
Complete devil staircase

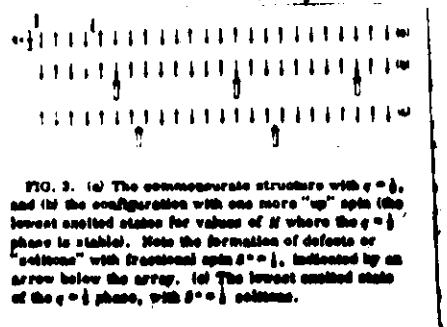

FIG. 2. (a) The commensurate structure with $c = \frac{1}{3}$, and (b) the configuration with one more "up" spin (the lowest excited states for values of H where the $c = \frac{1}{3}$ phase is stable). Note the formation of defects or "solitons" with fractional spin $S^z = \frac{1}{6}$, indicated by an arrow below the array. (c) The lowest excited state of the $c = \frac{1}{3}$ phase, with $S^z = \frac{1}{6}$ solitons.

Ground state of a 1-D chain with repulsive interactions (convex $V(r)$, $\frac{d^2V}{dr^2} > 0$)

- If $c = \frac{p}{q}$ (rational number) : place a particle at the origin
  - another at $\left[\frac{1}{c}\right]$
  - another at $\left[\frac{2}{c}\right]$ etc...

$[x]$ = INTEGER PART OF x

This leads to a periodic structure with period q and with p particles per unit cell

ex.: $c = \frac{2}{5}$ O-O--O O A • vacant site

- Another way to get the same structure for rational c values and for irrational values
  - introduce the crenel function $p(x) = 1$ if $\frac{a}{c} < x + b < \frac{a}{c} + q$; b is arbitrary
  - place a particle at a site x each time $p(x_n) = p_n = 1$ otherwise $p(x_n) = p_n = 0$

2 APB energies in TM alloys and PI

a) ORIGIN OF THE LRO?

- The G.P.M allows to determine the V_n and shows that they are strongly decreasing with distances. In fcc lattices, $|V_1| \gg |V_2| \gg |V_3| \gg |V_4|$. It's then quite difficult to believe that PI such as V_{100} V_{110}... can stabilize long periods. at T = 0K However, it's interesting to note that the APB energy ξ is zero on lines of the structural maps (calculated with $V_n = 0$ $n > 4$) b) the TM alloys for which "long" periods have been observed (Pt_3V; $M = \frac{q}{2}$, 2...) Pt_3Ti... Pt_8Ti) Pt_3Fe $M = 2$) are near these lines of ξ : this suggests that the long periods which have been observed are stabilized by entropy effects but the pb is still open !

b) HIERARCHY OF PI.

- We can then define a hierarchy of V_n according to the energy scale we are interested in:

$\Rightarrow$
- V_1 determines the order of magnitude of ΔE_{ord}
- V_2, V_4 det the nature of the stable O.S.
- V_3, V_5 det the interaction between APB and (?) the existence of T = 0K LRO APB structure

c) VARIATION OF ξ WITH BAND FILLING

- In practice, the antiphase boundary energy ξ must change of sign with the band filling (see fig and moments!). It can be estimated from the GPM. (Ni Fe alloys for example)

d) VARIATION OF ξ WITH LOCAL ORDER (T) - ANISOTROPY.

The A.P.B are usually observed at (high) temperatures; they play an important role in relation with the mechanical properties of alloys. The formulas we gave previously are valid at 0K - $\xi(T)$ is varying with temperature via the short range order parameters. For example above the order-disorder temperature the energy is:

$$\begin{cases} \gamma_{\frac{a}{2}}[1,7,0](111) = \frac{1}{\sqrt{3}} \frac{c_A c_B}{a^2} \big[(-2d_1 + d_2 + d_3) V_1 + (0, -3d_2 + d_3 + d_4) V_2 + \\ \qquad + (0, +d_2 - 9d_3 + 2d_4 + 3d_5 + d_6 + d_7) V_3 + \\ \qquad + 2 (d_3 + 3d_4 + d_5 + d_6) V_4 \big] \\ \gamma_{a\,(\text{cont})(111)} \end{cases}$$

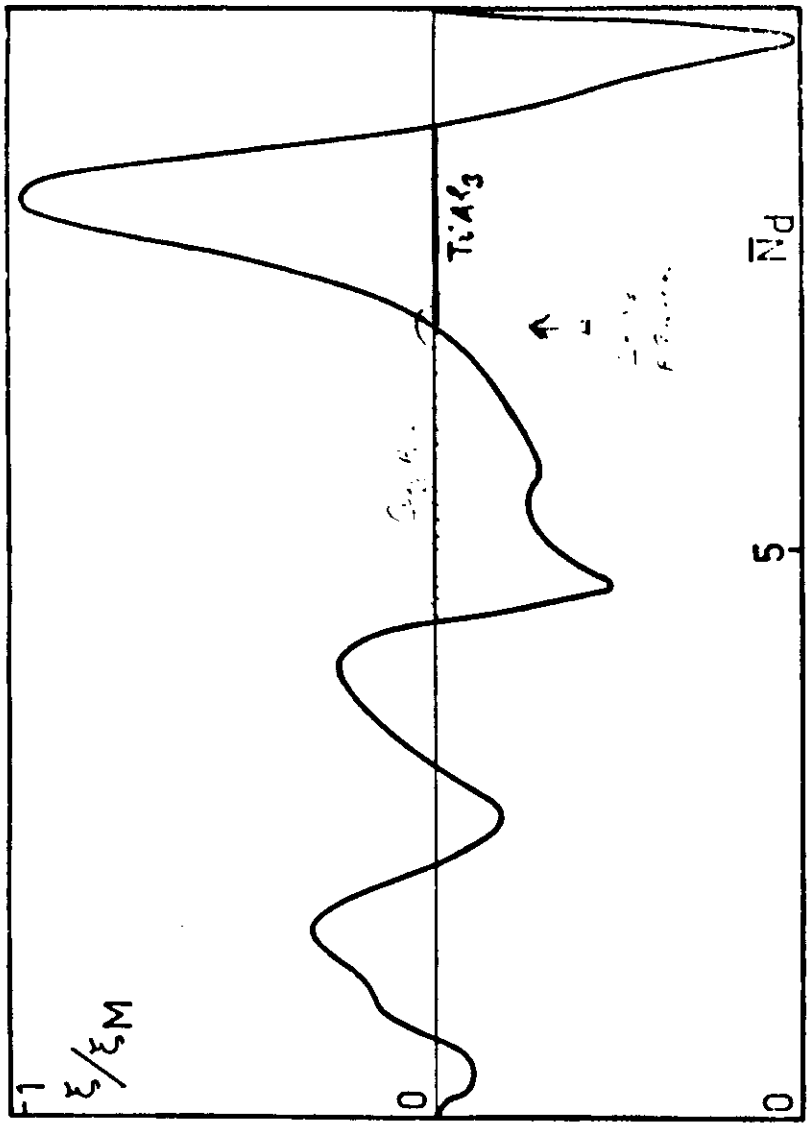

WE CONSIDERED PREVIOUSLY THE SIMPLEST CONSERVATIVE A.P.B. NEVERTHELESS IT'S IMPORTANT TO NOTE THAT THE ORDER INDUCES A STRONG ANISOTROPY OF THE LOW. ENERGY AS ILLUSTRATED BY THE FOLLOWING EXAMPLES

Ex - APB. (fcc) anisotropy

(1) $\gamma_{\frac{a}{2}[n\,\bar{n}\,0](111)} = \frac{1}{\sqrt{3}\,2a^2}\left(V_1 - 3V_3 + 4V_5 - 6V_6\right) \times$
$\times \left[\left(g^{(1)} - g^{(3)}\right)^2 + \left(g^{(2)} - g^{(4)}\right)^2\right]$
(ODD n)

T ≠ 0K

(2) $\gamma_{\frac{a}{2}[0,0,n](100)} = \frac{1}{(2a)^2}\left(-V_2 + 4V_3 - 4V_4\right) \times$
$\times \left[\left(g^{(1)} - g^{(3)}\right)^2 + \left(g^{(2)} - g^{(4)}\right)^2\right]$
( )

In Ni_3Fe :

(Th) $\begin{cases} \gamma_{(1)} = 186\ mJ/m^2 \\ \gamma_{(2)} = 41\ mJ/m^2 \end{cases}$ via P.I. exp 133 mJ/m^2

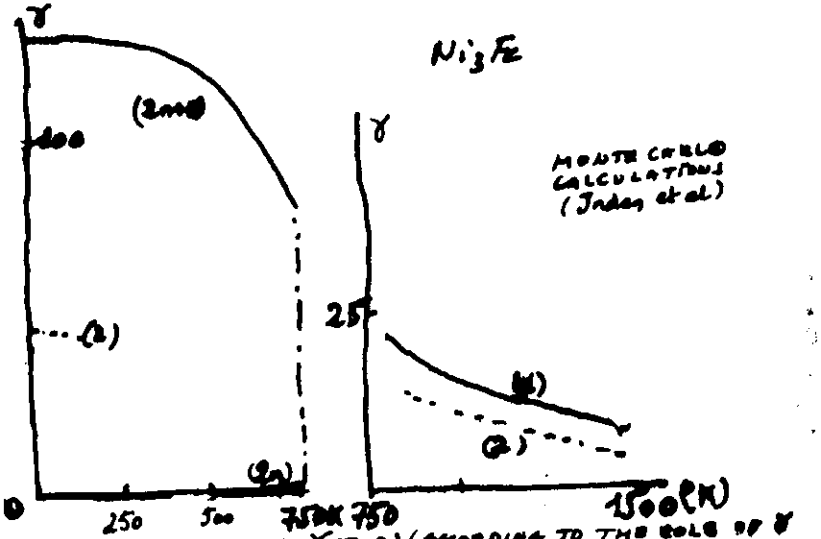

- STRONG ANISOTROPY OF THE $\gamma(T=0)$ (ACCORDING TO THE ROLE OF $\vec{g}$)
- DECREASES WITH INCREASING TEMPERATURE

GROUND STATE PHASE DIAGRAMS

Up to now, we considered only the relative stability of O.S (homogeneous states) at constant volume Ω. The determination of phase diagrams needs to relax these assumptions. We discuss in the next two pages the steps which are necessary to get such diagrams. Let us only point out here that (i) there is usually a competition between the elastic energy $\Delta E_{el} > 0$ and the chemical energy ΔE_{chem} so that, usually, for large difference in size this term induces segregation even if $\Delta E_{ord} < 0$ (ii) in most of the systems for which ΔE_{el} is not negligible ΔE_{el} modifies somewhat the sequence of O.S predicted by ΔE_{chem} only. More information will be found in the paper to be published in Acta Met. Some of them are given below.

PROGRAM FOR A CALCULATION OF THE PHASE (STABILITY) T=0K DIAGRAM

1 • TAKE INTO ACCOUNT THE IN SITE STRAINS ⇒ ΔE_{el}

2 • TAKE INTO ACCOUNT HETEROGENEOUS MIXING OF A WITH B CONCENTRATIONS

3 • TAKE INTO ACCOUNT DIFFERENT LATTICE (i.e., BCC, HCP, A15, L1$_2$, complex ...)

??

1 + 2 up to now...

FORMATION AND MIXING ENERGIES : VOLUME CHANGE

1. $\Delta E = \Delta E_{el} + \Delta E_o + \Delta E_{rel}$ ΔE_{chem} = "chemical"
$= \Delta E_{chem} + \Delta E_{el} + \Delta E_{rel}$

ΔE_{el} : ENERGY NECESSARY TO EXPAND (or COMPRESS) THE PURE CONSTITUENTS FROM THEIR EQUILIBRIUM AT VOL Ω_i TO THE ALLOY VOLUME Ω_Z (single phase φ)

$$\Omega_Z = c_A \Omega_A + c_B \Omega_B$$

ΔE_o MIXING ENERGY TO OBTAIN A GIVEN ATOMIC CONCENTRATION DISTRIBUTED ON THE PERFECT AVERAGE LATTICE WHOSE VOLUME IS Ω_Z

$$\Delta E_o = \Delta E_{dis} + \Delta E_{ord}$$

ΔE_{dis} IS THE CORRESPONDING ENERGY FOR A COMPLETELY DISORDERED CONFIGURATION

ΔE_{ord} IS THE "ORDERING ENERGY"

BOTH ARE CALCULATED USING G.P.M.

ΔE_{rel} RESULTS(4) FROM THE RELAXATION FROM Ω_Z TO THE ACTUAL VOLUME Ω_{Ac}) $\Delta E^{(1)}_{rel}$ (4) FROM THE ATOMIC DISPLACEMENTS FROM THE AVERAGE LATTICE (DISORDERED STATE) $\Delta E^{(2)}_{rel}$

$$\Delta E_{rel} = \Delta E^{(1)}_{rel} + \Delta E^{(2)}_{rel}$$

- V_i ... calculated ... back ... ab initio band structure calculations
- ΔE_{dis} is calc. from the CPA reference medium + multiple interactions (corrections)
- ΔE_{ord} is calc. from G.P.M. effective pair interactions

$$\Delta E_{ord} = \sum_i p_i V_i - \frac{c_A^2}{2} \sum z_i V_i$$

A = minority atoms ($c_A < 1/2$)

p_i = number of A pairs of i^{th} nn (per at)

z_i = coordination number

$$V_i^{\phi} = \overline{W}(c)\, V_i^{\phi}(c, \delta(c), \overline{W}(c))$$

$$\begin{cases} \overline{W}(c) = c_A W_A + c_B W_B(\Omega_2) \\ \delta(c) = 2\,\dfrac{\epsilon_A(c) - \epsilon_B(c)}{\overline{W}(c)} \end{cases}$$

Volume effects

- $\Delta E_{rel}^{(1)}$ by perturbation theory
- $\Delta E_{rel}^{(2)}$? needs the knowledge of {phonon spectra (?) and dipolar tensor and ?}

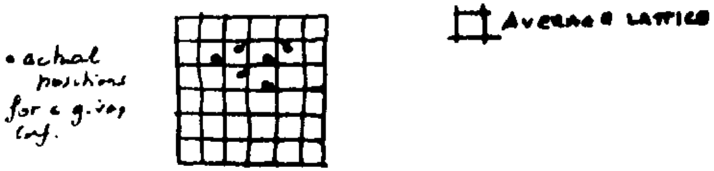

Such calculations have been done for different types of ϕ diagrams

Sc Nb	NbW	Ti Ta
Sc Mo	Tc Os	V Ru
Ti Mo		V Rh
Sc W		V Pd
Tc [illegible]		Sc Re
Ti Pt		Ti Re
[illegible] Pt		Sc Os
"[illegible]"	"Mi[illegible]"	Ti Os
		Ti Ir
		V Ir
		Ti Pt
		Mo Re

Qualitative discussion of the results for ΔE_{ch}

- The concentration dependence is quantitatively important (mostly for $\Delta E_{dis}(c)$) but qualitatively, the most stable homogeneous states (structural maps) are insensitive to the $\delta(c)$ variation

Deviation from a classical Ising model (role of ΔE_{dis}, V_i)

- There is no relation between ΔE_{dis} and ΔE_{ord} ($|\Delta E_{dis}|$ is in general much larger than the values deduced from a classical Ising model with the calculated P.I.

'Prototype diag'

- Three typical behaviours for $|V_2(c)|$
  - maximum value for $c \sim 0.5$ (VRh)
  - regular decr (increase)
  - change of sign

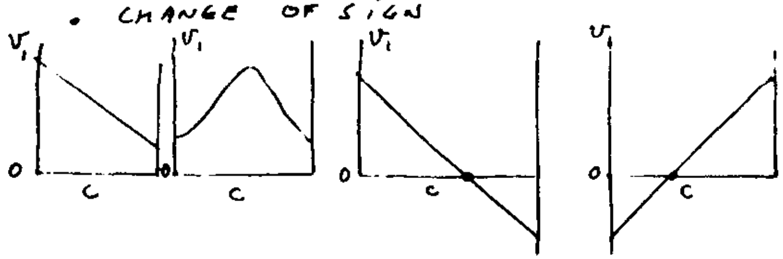

which will correspond to ≠ prototype diagrams but the role of $\Delta E_{el} + \Delta E_{dis}$ must be also investigated

(see A. Bieber F. Gautier: Acta Met 1987)
(see Turchi, de Fontaine et al (Phys Rev 1987) Sr T ≠ 0 K)

"TYPICAL SITUATIONS"

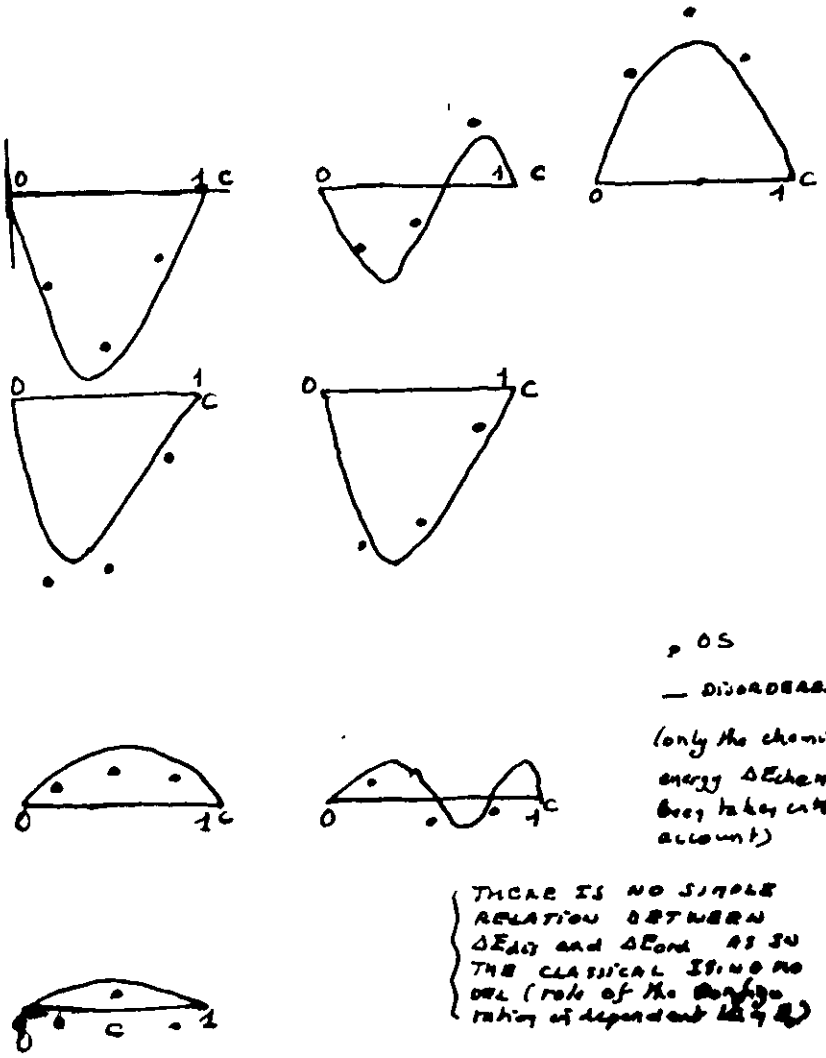

p OS

— DISORDERED

(only the chemical energy ΔE_{chem} has been taken into account)

THERE IS NO SIMPLE RELATION BETWEEN ΔE_{dis} and ΔE_{ord} AS SO THE CLASSICAL SEMI-EMPIRICAL ROLE (role of the bonding nature is dependent [illegible])

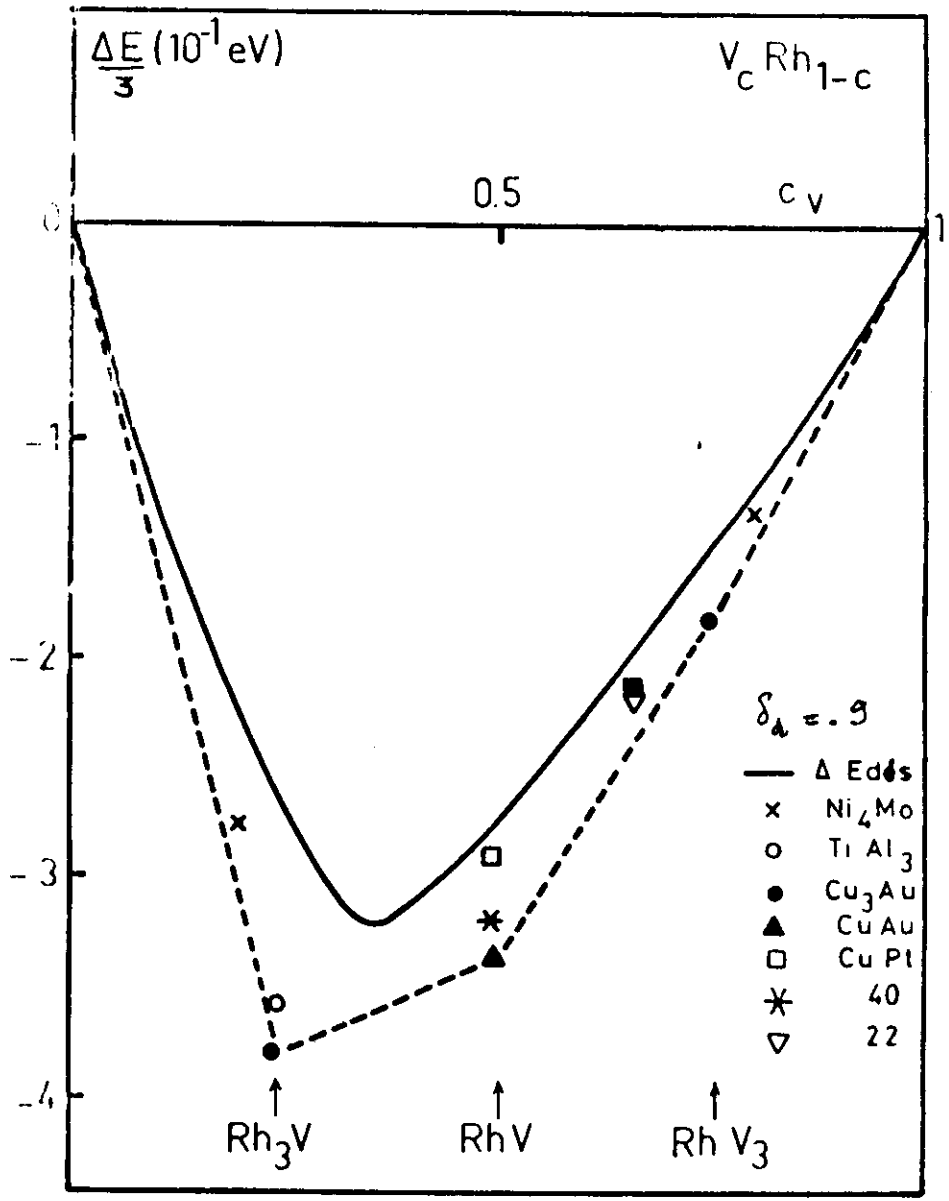

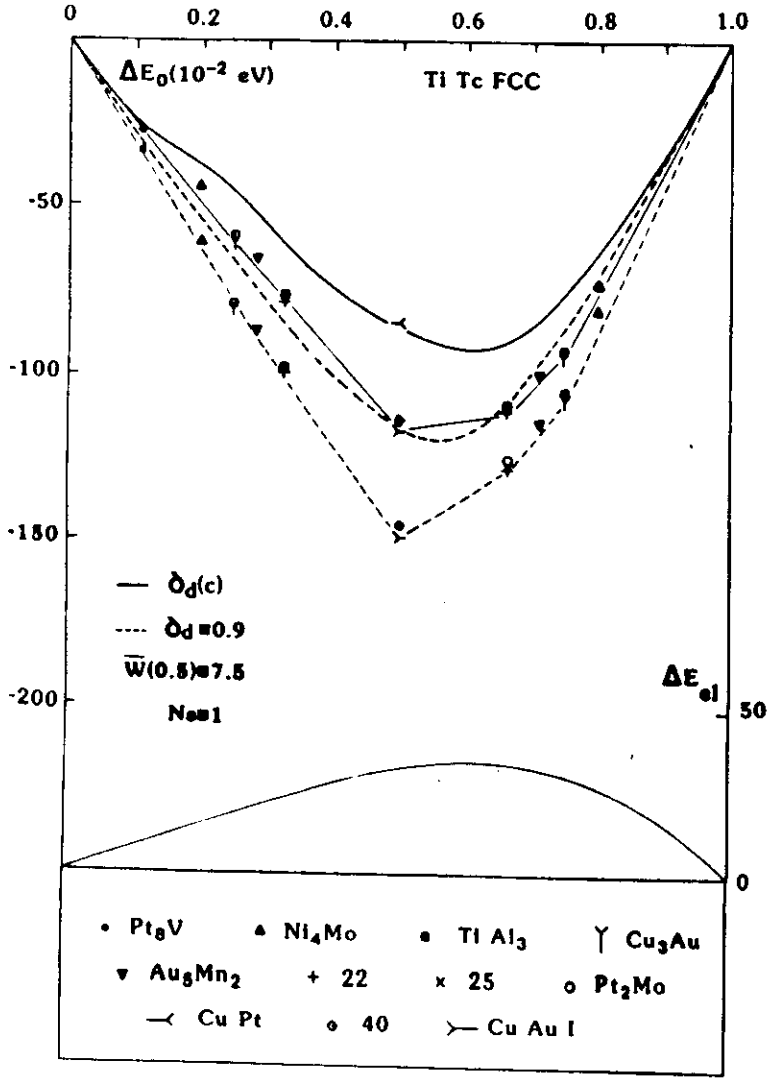

- NOTE THAT THE CHANGE OF δ WITH δ_{DOS} NOT CHANGE THE SEQUENCE OF O.S.
- THE QUANTITATIVE IMPORTANCE OF ΔE_{el}

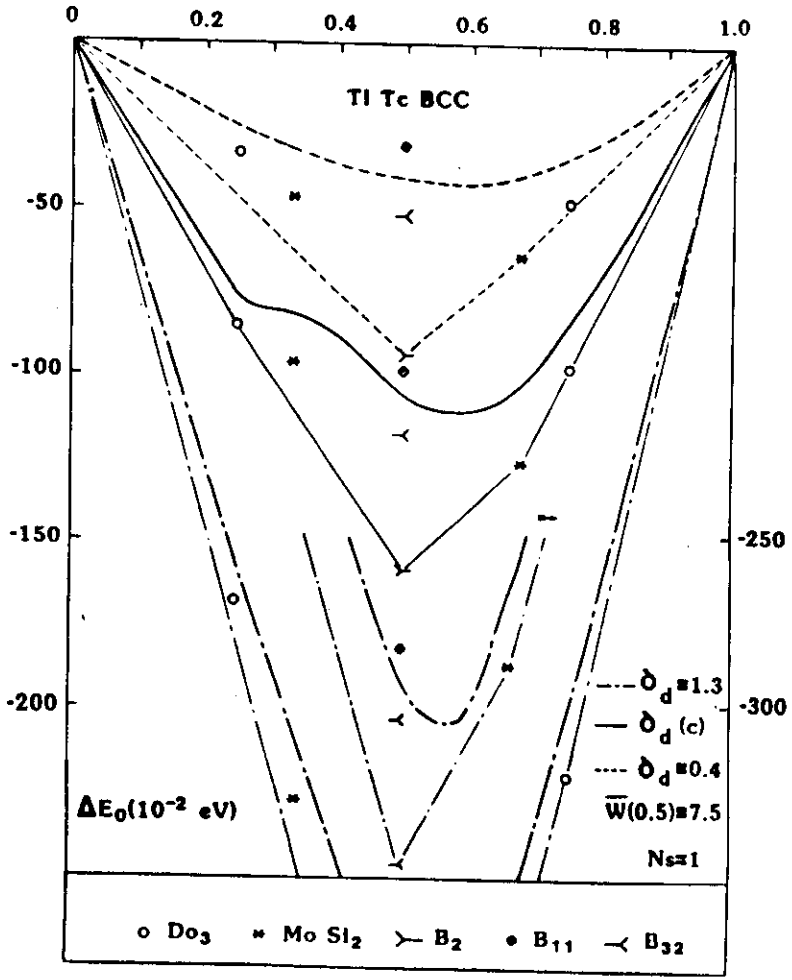

NOTE THE IMPORTANCE OF THE MAGNITUDE OF $\delta_d(c)$ ON THE RESULT! $\delta_d = 0.4$ and 1.3 ARE EXTREME VALUES OF $\delta_d(c)$.

3 PHASE DIAGRAMS AND PHASE STABILITY.

1. Introduction

Up to now, we considered only T=0K calculations. The problem is now to introduce study the phase stability vs T. A complete phase diagram calculation must thus take into account of all the possible origins of the entropy which enter in the calculation of the free energies:

- configurational entropy S_{conf}
- vibrational entropy S_{vib}
- electronic entropy S_{el} (our el)
- magnetic entropy S_{mag}

This separation is somewhat arbitrary (for example, S_{mag} and S_{el} are calculated simultaneously when a band model for magnetism is valid - ie for TM alloys) but useful. The delicate balance between the various terms for the phases in equilibrium needs a priori a precise determination of such quantities. Up to now, apart for semi empirical calculations of ϕ diagr which use free energies interpolated from various experimental data, there is no complete calculation of phase diagrams for the T.M. alloys. In this section, we discuss briefly the simple methods which have been used up to now.

The simplest idea to determine "Ist principles ϕ diagrams" is: (1) take only into account the most important configurational term S_{conf} and determine it by Monte Carlo approximation or by the "Cluster Variation Method" (2) determine the energy (or enthalpy) from the electronic structure. This program has been achieved for (normal) alloys of simple metals (CA Mg)

It's more difficult for TM alloys:

- The GPM allows to determine "a priori" the cluster expansion for the energy in crystallographic systems
- A special method must be derived for liquid transition metal alloys for which a cluster expansion seems to be too slowly convergent.

This is why, up to now, only few calculations have been done. Apart from phenomenological calculations (using short ranged P.I) and trying to relate the variation of of the PI with distance to the topology of the diagram (ie prototype phase diagrams) (de Fontaine) for a crystallographic state, only one determination of the phase diagram with a typical PI derived from the electronic structure (fcc lattice) has been done. Moreover the first attempt to calculate self consistently the SRO, from the electronic structure in the liquid state has been done as 1986 (Hafner - Pasturel)

In this section we will discuss briefly:

- the determination of ϕ diagrams (crystallographic state) using phenomenological PI and CVM or MC.
- the determination of PI from SRO measurements
- the calculation of the liquid state of TM alloys.

2 CALCULATION OF PHASE DIAGRAMS USING CVM and MC METHODS (CRYSTALLINE Φ)

2.1 The use of "CVM" and the importance of S.R.O

• We will assume in this section, that the energy is determined by concentration independent and short ranged pair interactions. We will consider only the configurational entropy S_{conf}. For a completely disordered system, the configurational entropy is given by: (binary alloy):

$$S_{conf}(c) = -N_A k_B (c \log c + (1-c)\log(1-c))$$

This is obtained from $S = k_B \log W$ where W is the number of ways to distribute at random $N_A c$ at A and $N_B = N(1-c)$ atoms B. This Bragg Williams approximation (or point approximation) neglects the SRO in the alloy. It's a first approximation which is not sufficient to get a good topology of the phase diagram.

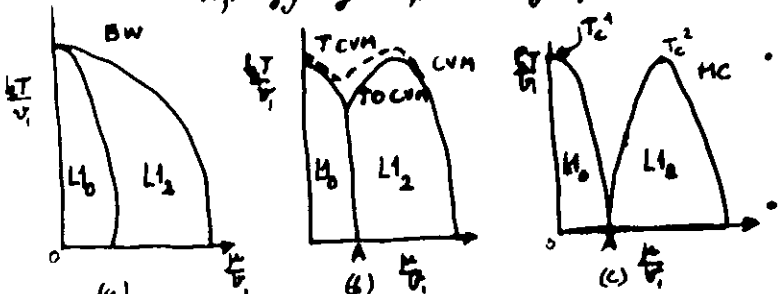

• HALF OF THE DIAGRAM IS REPRESENTED (it's symmetric with respect to μ or to c)
• THIS CORRESPONDS ROUGHLY TO THE Φ DIAGRAM [illegible]

(a). THE BWA IS NOT SUFFICIENT.
This is illustrated by the figure (a) which represents the phase diagram calculated using the BW approximation when we keep only 1st nn interactions v_1 ($v_n = 0, n>1$) and compared to the Monte Carlo calculation (fig (c)). This last calculation exhibits two different critical points for the phases $L1_0$ and $L1_2$ (T_{c1}, T_{c2}) and presents a topology which is in agreement with the exp. results for CuAu (except for the LP); its detailed shape is never-

-theless somewhat different from the experimental CuAu φ diagram shape (see the asymmetry and the change low temperature stability of "disordered phases near A. for the theoretical diagram whereas the experimental diagram is strongly asymmetric and does not present points similar to A.)

The cluster variation method is a way to determine the configurational entropy not only in terms of the "point" probabilities (c) but also in terms of cluster probabilities p_i, – $S_{conf} = S_{CVM}(\{p_i\})$ – which are chosen as independent variables characterizing the equilibrium state. The physical idea is to take into account the SRO which is important in a wide region around T_c and which is neglected in the BWA. The choice of the independent clusters for the evaluation of S_{conf} does not result from a systematic expansion but, from the physical idea that more accurate expressions of S_{conf} must take into account (more) larger compact clusters into account to represent more accurately the SRO. In the fcc lattice for example, the successive approximations will take into account the

"CVM"
- point — BWA — c only
- point + pair — Bethe — c, p_1
- " " + tetrahedra — c, p_1, p_2 p_3
- + octahedra — ....
- " " double tetrahedra — (cf fig.)

The energy is then written in terms of the same variables and the equilibrium state is obtained by minimizing $F = U - TS$. We don't describe here the way the S_{conf} can be written in terms of the p_i (see the De Fontaine review in Sol. St. Φ for example).

Let us note that the CVM is a mean field approximation: it neglects the fluctuations near the critical temperature. The

CVM AND DETERMINATION OF THE CRITICAL TEMPERATURES

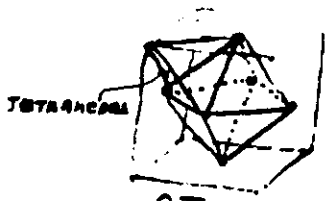

OT
Octaèdre tétraèdre.

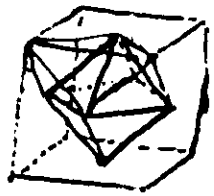

double tétraèdre octaèdre.

	$kT_c/12V$
Tetra	
DT	0.835
OT	0.840
DTO	0.834
⇒ ex.	0.830
{BW	0.816
{Bethe	1
	0.914

perature T_c (for a ferromagnetic system for example see Table p 36). Fig (6) (p 34) shows that the topology of the phase diagram for fcc lattice and V_1 only is recovered even of the point (2) above (stability of disordered phase at low T near A) is not recovered! In fact, this simple phase diagram is still contro versial in the A region and is somewhat pathological from the choice of the PI (V_1 only). The A point is then hyperdegenerate and the corresponding pathology disappears when we introduce a small $V_2 \neq 0$ value which lift the degeneracy -

The CVM is then a very simple mean field method which "is thought" (except for special points) to be sufficient for the evaluation of the topology of a phase diagram. The numerical work can become heavy when the number of cluster probabilities becomes high so that the minimization leads to a huge number of non linear algebraic equations and ... to difficulties of convergence

2. Prototype phase diagrams

The idea is to understand qualitatively the relation between the topology of the phase diagram and the pair interactions which determine this diagram. The simplest case is to apply the V_1 and 2d nn PI $V_{(2)}$ and to study the relation between the topology of the phase diagram and the ratio $\alpha = V_2/V_1$. We know, from the ground state results, that the nature of the low temperature phases varies also strongly with α; we know also that such a study is not academic since a number of important alloys are thought to be reasonably approximated by this model.

for example, Al Zn – $V_1 < 0$, $V_2 < |V_1|/2$; Cu Au – $V_1 > 0$, $V_2 < 0$; Ni Mo ($V_1 > 0, 0 < V_2 < V_1/2$) ; Cu Pt $V_1 > 0$ $V_2/V_1 > \frac{1}{2}$ or $V_2 < 0$, $\frac{V_2}{|V_1|} > 1$)

A large number of ordered structures and type of phase equilibria can be obtained – quite surprisingly – by varying the single parameter α – This shows that the topology of the diagram is very sensitive to the PI we use. How are such diagrams sensitive to more distants (but smaller) PI ? For example, we showed that if TM V_4 is of the order of V_2 in fcc structures. We show some of these (prototype) diagrams in the following figure.

3 Phase diagrams and PI from the GPM

For transition metal alloys, it has been shown recently that the PI are strongly varying with concentration (chapter IV) with typical variations. Recent calculations extend the previous work to such a case (Turchi et al Phys Rev B to be published). We noted that when the V_n are α dependent

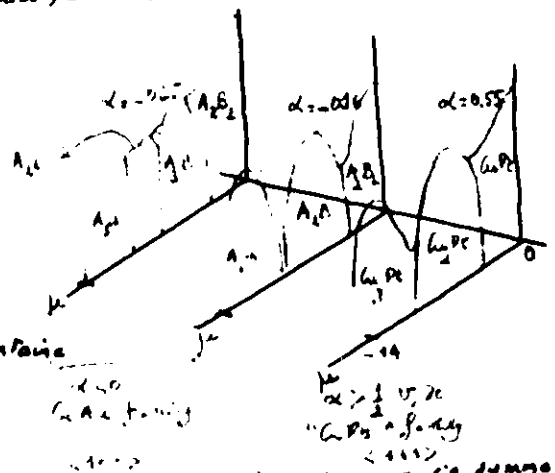

from D. De Fontaine (1988)

of the concentration, the phase diagram is symmetric with respect to $c = 0.5$ or $\mu = 0$ in disagreement with experiment. The variation of V_n with c allows to recover of a natural way this asymmetry. Note also that for strongly concentration dependent V_i the topology of the "Cu Au" phase

diagram is changed and new regions with phase segregation appear. Let us mention finally that this asymmetry has been first interpreted in Cu Au by multicritical interactions.

4 CVM ϕ diagrams : application to superalloys (Sanchez 1985)

In practice, for a number of alloys of metallurgical interest a first approximation using the BWA has been used, but some caution is required as shown by the first example (BWA for V_2 only on a fcc lattice).

In some cases, it's necessary to introduce phenomenologically a concentration (or volume dependence) of the PI to be in agreement with some experimental data. It's interesting to mention in this respect the work of Sanchez et al on Ni-Al and its alloys in relation to the superalloys. A constant pair interaction cannot reproduce the γ/γ' phase boundaries (γ disordered solid solution, γ' Ni_3Al_2) whereas phenomenological (8-4) Lennard Jones potentials allow to get a much better agreement. Note that the PI which enter in the calculation are thus concentration dependent via the

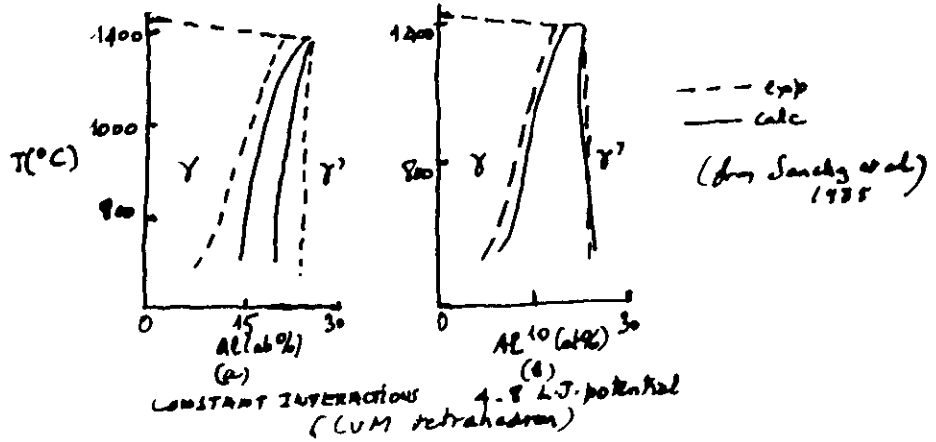

CONSTANT INTERACTIONS 4-8 L.J. potential (CVM tetrahedron)

corresponding dependence of the atomic volume.

This phase diagram and the corresponding LJ interactions differ

L.P CAN BE OBTAINED AT T=0K IN THE AXIAL AN NNNN MODEL WE USED IN ORDER TO EXPLAIN OBSERVED LONG PERIODS IN Cu Pd ALLOYS

(SCHEMATIC)

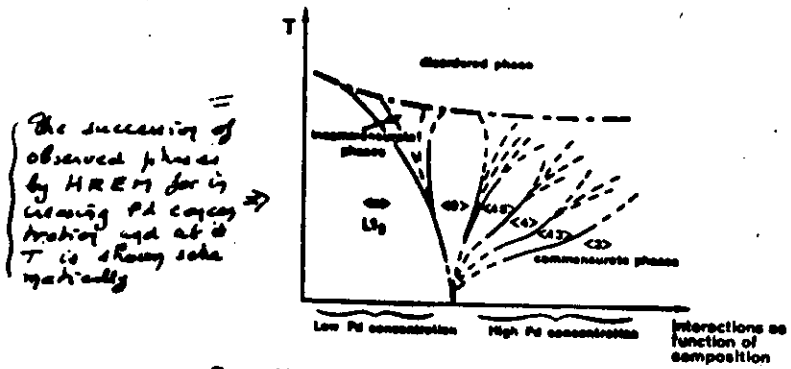

The succession of observed phases by HREM for increasing Pd concentration and at low T is shown schematically

Transposition of a qualitative ANNNI model suggested by de Fontaine and Kulik (1985) for Cu-Au; the x axis represents interactions depending on the Pd composition, which are not specified. The phases stabilized at low T are the $L1_2$ phase at the left of the multiphase point (low Pd concentrations) and modulated commensurate structures at the right (high Pd concentrations). At high temperatures, all the structures become incommensurate. Only incommensurate phases above the $L1_2$ structure are observed at low Pd concentrations since at high Pd concentrations the one-dimensional long-period superstructure transforms into the two-dimensional long-period superstructure at high temperatures.

(from A Loiseau et al Phil Mag 1986)

b) PHASE STABILIZATION OF LP BY ENTROPY EFFECTS

Schematic phase diagram for the ANNNI model in

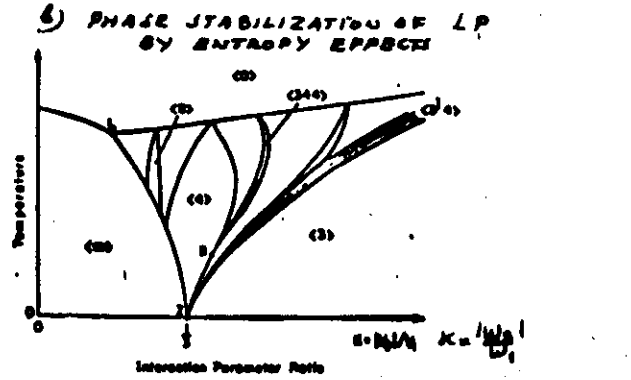

Fig. 52 (d'après [177])

- Schematic ANNNI model phase diagram with (V1,V2) interactions. L is Lifshitz point, I is multiphase point, B is one possible branching point.

from De Fontaine et al 1983)

Here, only interactions between 1st and 3rd nn neighbours have been taken into account (see the discussion p 18 →)

Structures ⟨2,1⟩ were observed if we retain only interactions between 1st and 2d nn

NOTE THAT THE TWO ACTUALLY [illegible]

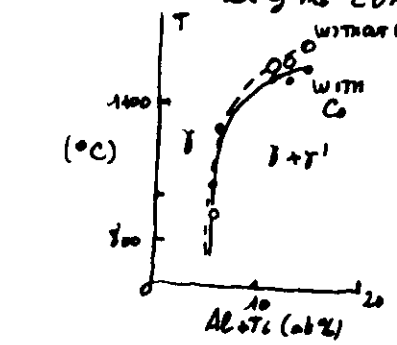

cpp γ phase boundaries for cobalt and cobalt free superalloys

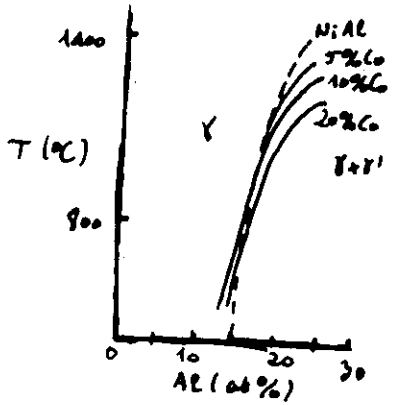

Theoretical CVM (Khachaturyan) calculations of the effects of Co addition on the γ phase boundaries in Ni Al

(from Sanchez et al 1985)

ROLE OF MAGNETISM ON THE ϕ DIAG

THE CHANGE IN TOPOLOGY OF THE ϕ DIAG

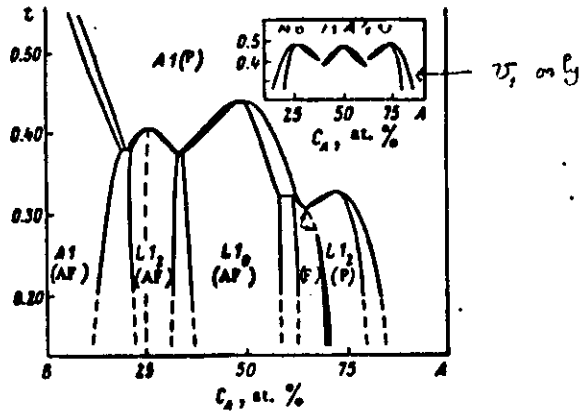

FIG. 2. Order–disorder phase diagram of A–B system in which B atoms have antiferromagnetic interaction ($J = -V/2$). Ordinates: temperature in units kT/V; abscissa: concentration c_A of nonmagnetic component. AF, F, and P denote antiferromagnetic, ferromagnetic, and paramagnetic phases. The arrows mark the second-order transformation curve.

Fig. 78a | (d'après |204|)

THE INTERPLAY BETWEEN X and magn INTER^{ON}

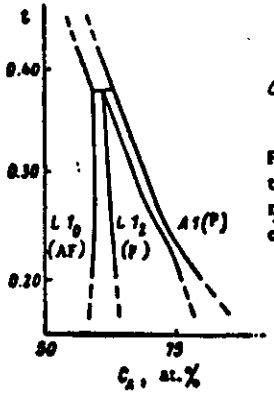

chemical / magn interactions

FIG. 6. Order–disorder transformation diagram calculated for ferromagnetic interaction in the second coordination sphere.

Fig. 78b | (d'après |204|)

CVM calculations fcc lattice (1st nn chemical and magnetic interactions)

Which Hierarchy + STRONG 1st nn FERROMAGNETIC INTERACTIONS BETWEEN TWO MINORITY MAGNETIC ATOMS IN AN ALLOY A_3B
+ SMALL J INTERACTIONS BETWEEN 1st and 2d nn A atoms
+ NO MAGN ON B ATOMS : EX. Pt_3Mn

THE $L1_2$ CHEMICAL ORDER (NO 1st nn AA pair) INDUCES A FERROMAGNETIC ϕ

3 Determination of the MAI from the short range order

The SRO is related to the MAI in an equilibrium state. This relation is quite simple in the lowest approximation (Clapp-Moss formula):

$$\alpha(k) = \frac{C}{1 - c(1-c)\tilde{V}(k)/kT}$$

where $\tilde{V}(k) = \sum_j V(j)\, e^{i k \cdot j}$ is the lattice Fourier transform (FT) of the irreducible PI, C is a constant determined to satisfy a sum rule (see de Novion Lechaux) and $\alpha(k)$ is the FT of the short range order parameters defined in chapter 1. This formula (analogous to the Curie Weiss law for magnetism) is an approximate formula which does not take (account properly) and self consistently of the SRO. Nevertheless, it shows how to get $\tilde{V}(k)$ and V_i (in principle) from a measurement of the SRO in alloys (diffuse neutron and X ray scattering). A reliable determination of the V_i from experiment is rather difficult both for experimental and theoretical reasons. From an experimental point of view, it's often difficult to do the experiments at equilibrium (quenching is often not always a good way!) so that, if we are out of equilibrium ... the measurements have no more meaning in relation with V_i. From a theoretical point of view the formula is not sufficient "a priori" so that it's necessary (!) to assume the nature of the relevant MAI (!) to solve by MC – or CVM – the SRO for given values of MAI and to get (unicity ?) the polynomial values for the MAI which fit to the experiment. This "inverse pb" is not easy to handle. In the next figure

	l	V_l(HT) (Clapp Moss)	V_l(MC inv) Monte Carlo
PAIRS	1	22.5	25.9
	2	-11.2	-10.9
	3	- 1.4	- 1.5
	4	5.0	5.0
	5	0.1	0.2
	6	- 0.3	- 0.18
	7	- 0.86	- 0.97
	8	- 1.1	0.8
	9	- 2.5	2.45
	10	- 0.3	
	11	- 0.17	
	12	- 1.1	
TRIPLES	$V^{(3)}(\pi/2)$		- 0.3±0.9
	$V^{(3)}(2\pi/3)$		- 0.9±0.6
	$V^{(3)}(\pi)$		- 4.8±2.1

(a)

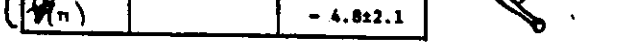

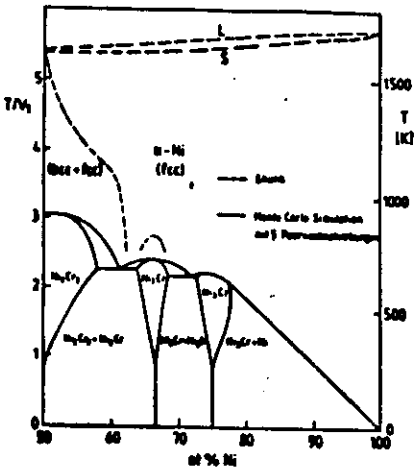

- VALUES FOR PAIR INTERACTIONS AND TRIPLET INTERACTIONS — AS INTRODUCED IN THE GIPM — ARE DEDUCED FROM M.C INVERSE METHOD (a) (neutron diff. scatt. exp.)
- THE MC PHASE DIAGRAM DEDUCED FROM TRUE MAIS IS SHOWN IN (b). IT'S NOT IN AGREEMENT WITH THE AVAILABLE PHASE DIAGRAMS (Ni$_3$Cr ?)

Note that the orders of magnitude of the V_l are consistent with the results of the GPM (chapter 4)

Very few experiments are available up to now (see De Novion lectures) but we note only here that (i) the relation $|V_2| > |V_1|$ suggested by the GPM analysis of order-disorder in Cu-based ternary alloys (de Fontaine et al) is verified by accurate neutron diffuse scattering (Q) a change of sign of the PI with concentration has also been shown by neutron diffuse scattering, a cross over between segregation and order occuring when we vary c (Mennion et al 1984)

4 THE TM and TM alloys in the liquid state.

We showed previously that - up to now - it's difficult to get a convergent cluster expansion for TM alloys with topological disorder. It's thus impossible (?) to use the classical methods of liquid theory to determine the radial distribution functions from the PI deduced themselves from the pseudopotential theory. A new method has been recently introduced and applied. Let us discuss it briefly.

1 The reference medium : THE HARD SPHERE YUKAWA MEDIUM

As usually, we will describe the system with T-SRO and C-SRO (T = topological ; C = chemical) by a perturbation from a REFERENCE MEDIUM. The simplest way is to use the HARD SPHERE YUKAWA fluid which was used to study ordering in molten salts, liquid semiconductors and also in some metallic alloys - the order in this fluid characterized by hard spheres (charges Q_1, Q_2, radius $\sigma/2$) interacting via Yukawa pair potential ($\sim \frac{\exp -Kr}{r}$, K^{-1} is the Yukawa length) is deduced by Orstein Zernike equations for the partial structures and total correlations functions (see TOSI LECTURES). The interest of this model from a technical point of view is the decoupling

of the three integral equations defining the partial correlation functions $c_{ij}(k)$ (c_{NN}, c_{cc} are decoupled; the first one is determined by a Percus Yevick equation, the last one is known also analytically; $c_{Nc}=0$ in the Bathia Thornton notation) the ij dependent parameters which determine the order are:

σ = HARD SPHERE DIAMETER, $\epsilon = -c_A c_B (Q_A - Q_B)^2$ = FLUCT OF CHARGES, κ^{-1} = YUKAWA SCREENING LENGTH.

the free energy of the HSY model:

$$F_{ref}(\epsilon, \kappa, \sigma) = \frac{3}{2} kT + \Delta E_{ord}^{ref} - T(S_{HS} + \Delta S_{ord})$$

S_{HS} is the well known hard sphere entropy, $\Delta E_{ord}^{ref} = \frac{c_A c_B w}{2}$ where w is related by a quadratic equation to σ, κ and ϵ. ΔS_{ord} is also analytical. The important point is that the free energy is analytically defined in terms of σ, ϵ, and κ, so that minimization procedures will be easier.

2. The electronic energy. (band energy) BETHE LATTICE APP

The electronic energy for the TM alloys is represented by a T.B model and various approximations must be introduced to get a reasonable assumption on the electronic structure of such topologically and chemically disordered systems. The local (configurationally averaged) density of states (and Green functions) is assumed to a function of the partial coordination numbers Z_{ij} (for a crystalline state) ($Z_{AA} = Z_1 c + (1-c) z_2$, $Z_{AB} = Z(1-c)$, $(1-2)$ in the usual notation) only. This is given by:

$$\eta_i(\epsilon) = -\frac{1}{\pi} \frac{\Delta_i}{(\epsilon - \epsilon_i - \Delta_i)^2 + \Delta_i^2} \qquad \Delta_i = \frac{z_{ii} t_{ii}^2}{\epsilon - \epsilon_i - \Delta_i} + \frac{z_{ij} t_{ij}^2}{\epsilon - \epsilon_j - \Delta_j}$$

$\Delta_j = \frac{\Delta_i(Z_{ij})}{Z}$

these simple equations are deduced from an alloy Bethe lattice approximation we don't describe (F. Brouers et al in "Amorphous magnetism p. 151 (1973). Their interest is to

take into account in the simplest way the effect of the local environment on the local densities of states.

These formulae must be modified to take into account the atomic structure in the liquid state. We thus skip the replacement: $z_{ij} t_{ij}^2 \to n_a \int g_{ij}(r') t_{ij}^2(r') dr'$ where, as usual, the g_{ij} are the partial distr. functions. (bound resp.) Eo Left the concentration on the integral, it's assumed to be infinite in the previous formulae $\Delta_i = \Delta_i$ and the Δ_i are given by very simple formulae:

$$\Delta_A = \frac{n_a c_A \int t_{AA}^2(R) g_{AA}(r) dr}{\epsilon - \epsilon_A - \Delta_A} + \frac{n_a c_B \int t_{AB}^2(R) g_{AB}(r) dr}{\epsilon - \epsilon_B - \Delta_B}$$

+ a similar equation $A \leftrightarrow B$.

For TM the t_{ij} are assume to vary as $t_{ij}(R) = t_{ij}^0 \exp -q R$ ($qR_0 \times 3$ - where R_0 is the 1st nn).

We assume also that the total band sphere volume does not change with alloying; σ is then fixing the mean atomic distance and it's no more useful to introduce a repulsive energy for the electronic energy in the variational procedure as shown below.

3. The variational procedure.

As usual we use, as liquids the Bogoliubov inequality

$$F \leq F_{ref} + \langle \mathcal{H} - \mathcal{H}_{ref} \rangle_{ref}$$

where F_{ref} is the reference free energy and the second term represents the average (thermal av. for $\mathcal{H}_{ref}$) of the perturbation. In the present case:

$$F \leq F_{HSY} + \langle \mathcal{H} - \mathcal{H}_{HSV} \rangle_{HSY} =$$
$$= \frac{3}{2} kT + E_T(\epsilon, \kappa, \sigma) - T S_{HSY}(\epsilon, \kappa, \sigma)$$

E_T is the band energy we discussed in 2.

For simplicity, the HS diameter is determined by fitting the excess entropy of the supercooled pure liq. metals and a complete minimization of the free energy has not been done yet on the replacement of the individual hard sphere diameters by an average value or limits the applicability of the calculations to systems for which size effects are small. - The ϵ and κ values are then obtained by minimization of the model free energy

The preliminary results on $Ti_{40}Ni_{60}$ and Zr Ni alloys are very encouraging. For Ti Ni alloys

- The density of states of LTiNi is similar to the one we discussed previously for aTiNi but it is structureless and the pseudogap has been filled (partially) in LTiNi
- The partial structure factors $S_{NiNi}(q)$, $S_{CC}(q)$ compare very well with those of the deduced from neutron scattering data. S_{NiNi} is determined by the packing fraction η so that the comparison between exp and th must be focussed on S_{CC} which is a real prediction of the theory
- The amplitude of the 1st peak of S_{CC} depends on ϵ and κ
- The position of the peak $Q_1 = 1.58$ Å is almost insensitive to ϵ and slightly decreases with decreasing κ value

We show in the next figure the results of $S_{CC}(q)$ for Ni Zr alloys : the C.S.R.O. is shown to decrease strongly with increasing Zr composition in agreement with exp on amorphous systems

4 Liquid and amorphous alloys : two remarks

- Experimentally, the distribution functions for the supercooled liquid (just above the glass temperature) and the corresponding functions for a glass with the same composition are very similar - the most important difference

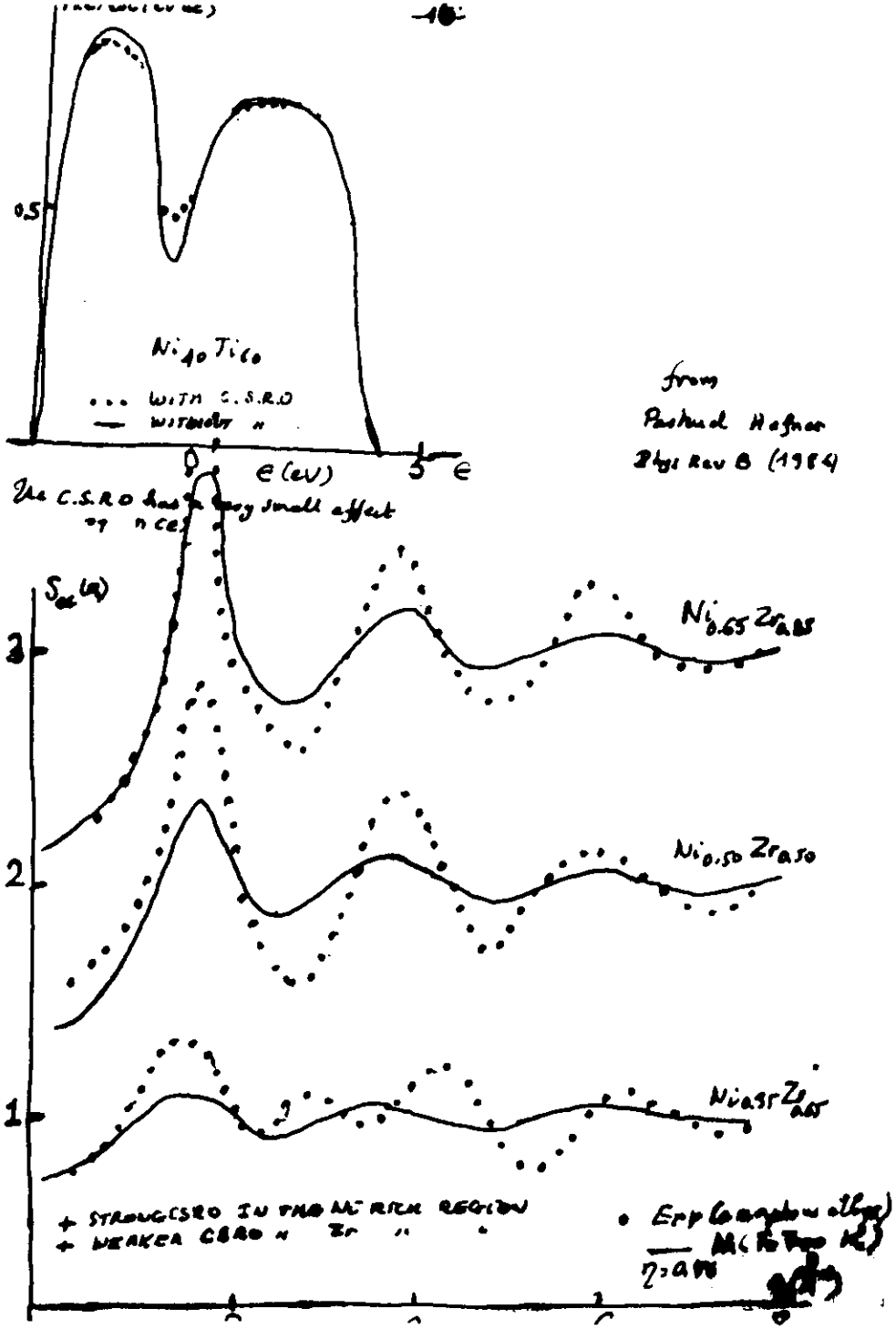

The study of cSRO in simple metal alloys by molecular dynamics techniques and by variational techniques similar to those used previously shows also a strong similarity - of Scc mostly - between amorphous and liquid state. It's thus tempting to assume that both are the same in glasses and liquids.

- This chemical SRO can be rather complex. The energies necessary for ordering such alloy being larger than those which are considered for changes of topological order (see chapter II), it's thought that the C.S.RO in glasses is similar to the one which is observed in O.S with the same composition. When the composition of the glass is different from the composition of the stable (or metastable OS), we expect to find a complex C.S.RO which is a "mixing" between two SRO characteristic of the considered compounds. This has been shown experimentally by NMR experiments on metal metalloïd alloys (NiB is an example)

5 THE IMPORTANCE OF PRECISE DETERMINATIONS OF THE ENTROPY TERMS FOR THE CALCULATION OF PHASE DIAGRAMS

1 Introduction.

We pointed out in the previous section that the topology of the phase diagrams can be changed if a proper account of C.S.RO effects is taken (using model with only 1st nn V_i PI in the BNA as compared to the MC results). Let us now discuss another example which is important for a better study of glass forming : the Au-Si system. This system has a complex ϕ diagram characterized by an eutectic whose temperature T_{eu} is very low. ($\simeq 340°C$). The thermodynamic work by Castanet showed that this eutectic cannot be reproduced by an ideal liquid free energy (see fig) - The low value for T_{eu} comes from a strong decrease of ΔS_{liq} with decreasing temperature (see fig) which is probably related to an increase of chemical SRO short range order for c.c.o.s. Note that the eutectic results from the equilibrium between the pure elements and the liquid : the value of the concentration of the eutectic c_{eu} is thus related to the G values for the all the phases which determine the equilibrium. Neither T_{eu} nor c_{eu} are characteristic only of the C.S.RO in the liquid phase. This example shows clearly the importance of a good estimation of ΔS - and notably here of ΔS_{conf} - to get reliable phase diagrams.

Au-Si ϕ diagr

It's important to note that the other contributions to ΔS can be equally essential for the calculation of phase diagrams. Several contributions are usually considered :

$$\begin{cases} \Delta S = \Delta S^{ideal} + \Delta S^{xs} & (1) \\ \Delta S = \Delta S_{conf} + \Delta S_{el} + \Delta S_{magn} + \Delta S_{vib.} \end{cases}$$

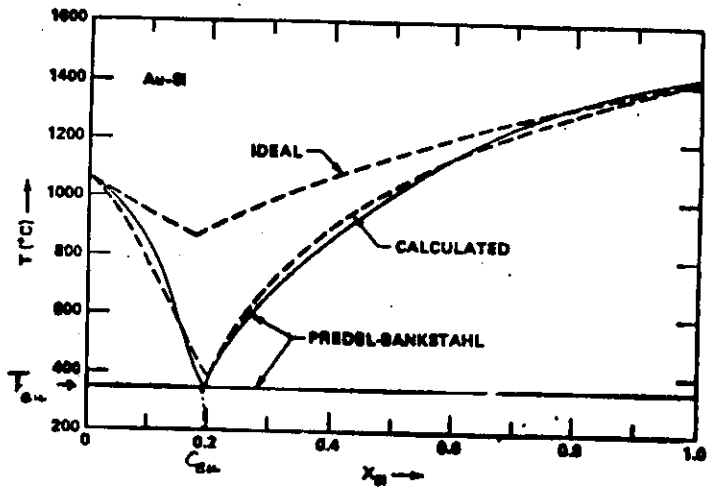

THE IDEAL ENTROPY CANNOT BE CONSISTENT WITH THE ϕ DIAGRAM

Comparison of Au-Si eutectic phase boundaries determined experimentally, calculated using the mixing free energy function of Castanet et al, and calculated for an ideal liquid.

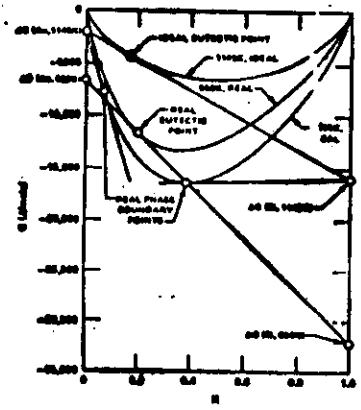

Figure 2.

The common tangent construction leading to the phase boundary shown in Fig. 1

ϕ EQUILIBRIUM DEFINING T_{Eu}, C_{Eu}

(from J. Alloys et al.)

Figure 4.

The composition and temperature dependence of the excess entropy of Au-Si liquid.

NOTE THAT THE ΔS VALUES ARE OF ΔS WHEN IT IS PROBABLY FROM

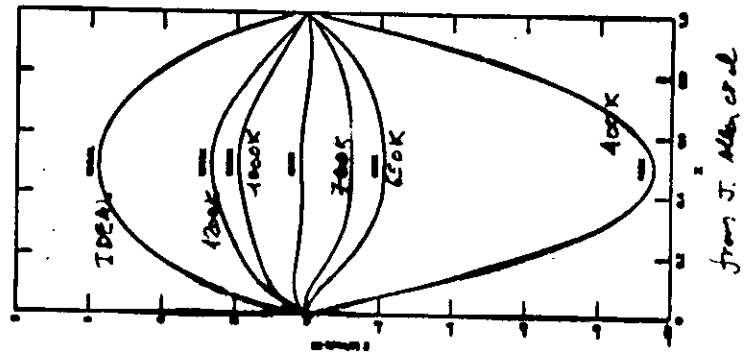

from J. Alloys et al.

The excess entropy ΔS^{xs} is defined by (1) where ΔS^{ideal} is the entropy which is determined in the BW approximation without taking in to account the SRO. $\Delta S^{xs}_{conf} = \Delta S_{conf} - \Delta S_{ideal}$ is thus the entropy which comes from the SRO.

Our aim here is not to present a general overview: it's only to select some examples which show that the contributions ΔS_{el}, ΔS_{magn}, ΔS_{vib} can introduce qualitative changes of the phase stability. A RELIABLE "1st PRINCIPLES" CALCULATION OF PHASE DIAGRAMS MUST TAKE INTO ACCOUNT THESE EFFECTS!!

2 ELECTRONIC ENTROPY

The electronic entropy is given by:

$$S_{el} = \frac{1}{3}\pi^2 k_B^2 n(\varepsilon_F) T \qquad \text{(see Kittel)}$$

for non interacting electrons and when $k_B T$ is not too large as compared with the scale of variation of the D.O.S. (Otherwise one replace $n(\varepsilon_F)$ by an average $\bar{n}(\varepsilon_F, T)$ of $n(\varepsilon_F)$ over a range $k_B T$ around $\varepsilon_F(T)$ Several corrections must be introduced to take into account of the correlations and of the interaction with vibrations: the formula (2) is nevertheless sufficient for a qualitative discussion.

a) ΔS_{el} and structural changes

It is generally assumed that this term is not important (as compared with ΔS_{conf}.) We want to point out that this is not the case in TM alloys for which usually $n(\varepsilon_F)$ is large (W small). We show, in the next figures, the change of entropy $\Delta S_{el}^{fcc \to bcc}$ and estimated values from different pure TM systems. This change in entropy results from ΔS_{vib} and from ΔS_{el} + ΔS_{magn} since we consider only changes in Topological order.

→ ΔS_{el} IS CHANGE OF TOPOL. ORDER

THE ELECTRONIC ENTROPY CHANGES $\Delta S_{el}^{hcp \to bcc}$ WHICH COMES FROM THE RELATED CHANGES IN THE DOS AT THE FERMI LEVEL ARE OF THE SAME ORDER OF MAGNITUDE AS THE EXP.

EXPERIMENTAL (or ESTIMATED) VALUES FOR $S_{hcp} - S_{bcc}$

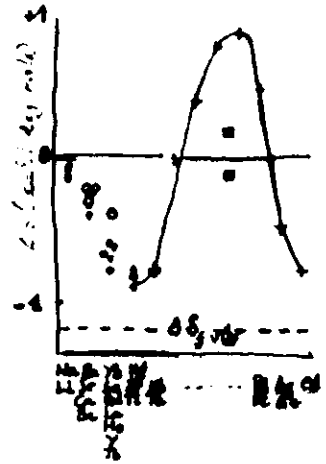

- $\Delta S^{hcp \to bcc}$
- $\Delta S^{fcc \to bcc}$ } from phase transitions
- $\Delta S(Fe)^{bcc \to fcc}$
- $\Delta S(Fe)^{fcc \to bcc}$
- + and from Kaufman and Bernstein (estimation from $\phi(r)$)

ΔS_{vib} = vibrational entropy term predicted by Moriel

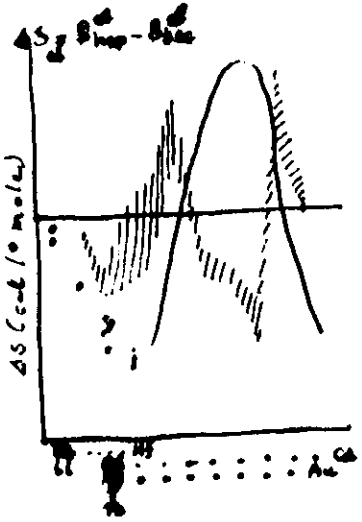

- THE ELECTRONIC ENTROPY HAS BEEN CALCULATED FROM THE BAND STRUCTURE OF Mo (Mattheiss)
- NOTE THAT IT'S OF THE SAME ORDER OF MAGNITUDE AS THE ESTIMATED AND EXPERIMENTAL VALUES

(from R.B. Watson & L.H. Bennett (1968))

RELATIVE STABILITY OF bcc AND hcp PHASES CAN THUS BEFORE OF A SUBTLE BALANCE BETWEEN VIBRATIONAL AND ELECTRONIC ENTROPY CHANGES (at high T) Note that a precise value of ΔS_{el} is not so easy to get in pure metals : the peaky nature of the DOS leads to uncertainties on $n(E_F)$ (as shown by a comparison between several band calculations) which are taken into account in the shaded area of fig p.

b) ELECTRONIC ENTROPY CHANGES IN "sp-d" ALLOYS

The electronic entropy can be also essential to the study of TM-TM or TM-sp systems. Let us consider as an example the case of liq. TM-Sp systems such as Fe Si Co Si Ni Si. They are characterized large negative by a heavy of mixing. (see below)

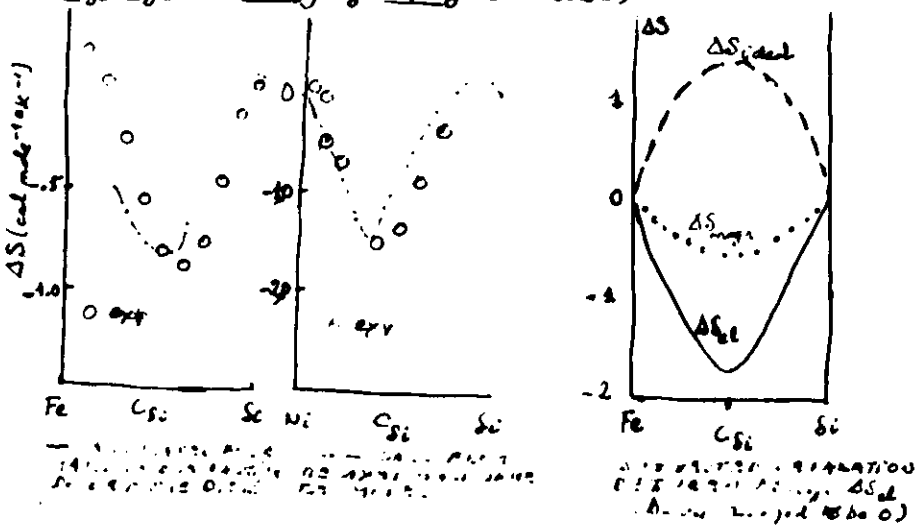

Vibrational entropies for different topological environments.

c) The origin of the negative lobe can be easily found by a qualitative argument valid for sp-d compounds : going from a TM (with a high density of states) to a normal metal (with a low density of states), the density of states is thought to be decreasing roughly linearly : it first decreases rapidly (filling of the d bands and then slowly when the band is filled). This leads to a strong negative ΔS_{el} value (see fig p 53)

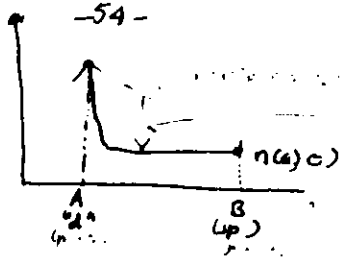

This qualitative argument is based on a rigid band model and must be checked in detail for each case. Nevertheless, a simple estimation of ΔS_{el} (based on non hybridized sp-d systems) and of ΔS_{mag} (assuming that the introduction of non magnetic elements is simply suppressing the corresponding site) give reasonable results

3 Vibrational entropy and phase stabilization

a) bcc vs compact structures

The vibrational entropy has been invoked from a long time (Zener 1947) to explain the larger stability of bcc structures (at high temperatures) than those of compact structures. Most of the high The number of observed bcc phases at high temperatures is much higher than the number of compact phases A first explanation is based of models which presume that the bcc structure is "softer" (with respect to shears) than the compact structures. Friedel estimated this effect using a simple phonon model : the corresponding value is shown on ΔS_{vib} in the fig giving $\Delta S^{hcp \to bcc}$ (p 52). A more complete calculation needs a detailed estimate of the phonon densities of states and of the anharmonic effects at high T.

Note finally that this experimental observation can be also easily deduced from a phenomenological Landau theory of solidification : the bcc structures appear in such a case like the isomorphous approximation whereas other structures appear (quasi) when higher order in the [illegible]

Up to now, there is no systematic effect of vibrational entropy effects in TM alloys. However, simple estimates based both on the phonon spectra of alloys and on the electronic structure (Moraitis-Gautier) show that they are relevant for a phase diagram calculation of such systems. A detailed discussion of these effects is out of the scope of these lect.

6 METASTABLE PHASES AND NON EQUILIBRIUM PHASES.

Modern materials are often (or perhaps always) out of equilibrium. It's thus of outmost interest to understand in more details the phase stability of such systems. It's possible to extend the concept of equilibrium phase diagrams by introducing the notion of metastable phase diagrams which identify the stability of order under well defined constraints. For example, in the case of artificial structures we discussed in chapter 1, it's possible to study the order in a layer interacting with the neighbouring layers, the diffusion being blocked across the interfaces.

The most studied metastable alloy phases are the amorphous alloys which can be obtained in a number of different ways (quenching from the melt, sputtering, solid state reaction etc...) Our aim, here, is only to discuss briefly some concepts which were developed for a study of the glass forming ability (GFA) and of the glass stability in relation with thermodynamic data. We limit these remarks to the formation of metallic glasses quenched from the liquid phases and we show that a careful examination of these data can lead to a satisfactory understanding (and prediction of the formation of glasses.

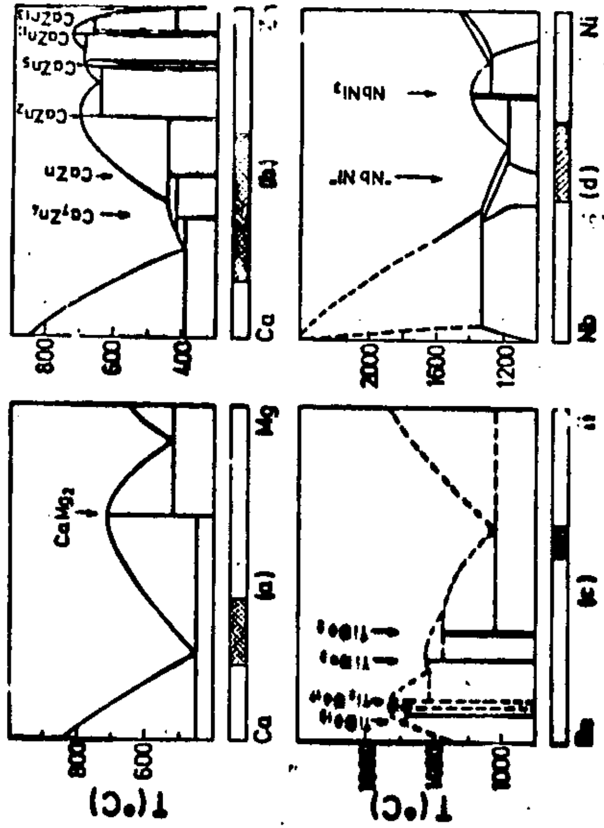

SOME TYPICAL PHASE DIAGRAMS WITH THE EXPERIMENTAL COMPOSITION RANGES FOR GLASS FORMATION

(from Ito...)

(Whetstone Ord (am))

Many phenomenological criteria for the GFA have been introduced. Some of them take into account the kinetics of the formation of glasses: the important parameter is then:

$$T_{gr} = \frac{T_g}{T_l}$$

and the critical cooling rate R_c necessary to get glasses increases rapidly with decreasing values of T_{gr} ($T_{gr} > 0.6$ for $R \sim 10^5\,°K\,s^{-1}$). In the previous formula T_g is the glass temperature and T_l the liquidus temperature.

Most of the usual criteria are related (perhaps naively) to the equilibrium phase diagrams:

— low eutectic temperatures $\frac{T_{eu}}{T_l} \leq 0.6$, and large mixing enthalpies ($|\Delta H_m| > 10$ kcal/mole), avoid solid solutions (large size effects ($\frac{R_a}{R_b} > 1.15$ for M-M glasses), large cohesive energies and formation energy for vacancies, ... have been invoked to favour glass formation — "Structural maps" similar to those which were introduced for equilibrium OS can be built for the GFA. (plot for example ΔH_m, r_A/r_B Giessen)

We discuss here the work by Hafner on Ca-Mg system in order to show that 1st pples φ diagrams can be used to get a reasonable prediction of the glass forming ability. This system is characteristic of those systems with weak chemical interactions and small deviation from ideality. The energetics of such systems and the GFA are governed by physical principles somewhat different from those of systems with strong chemical interactions, large deviations from ideality (as usually TM-TM systems). These two limiting cases will be opposed in the following discussion.

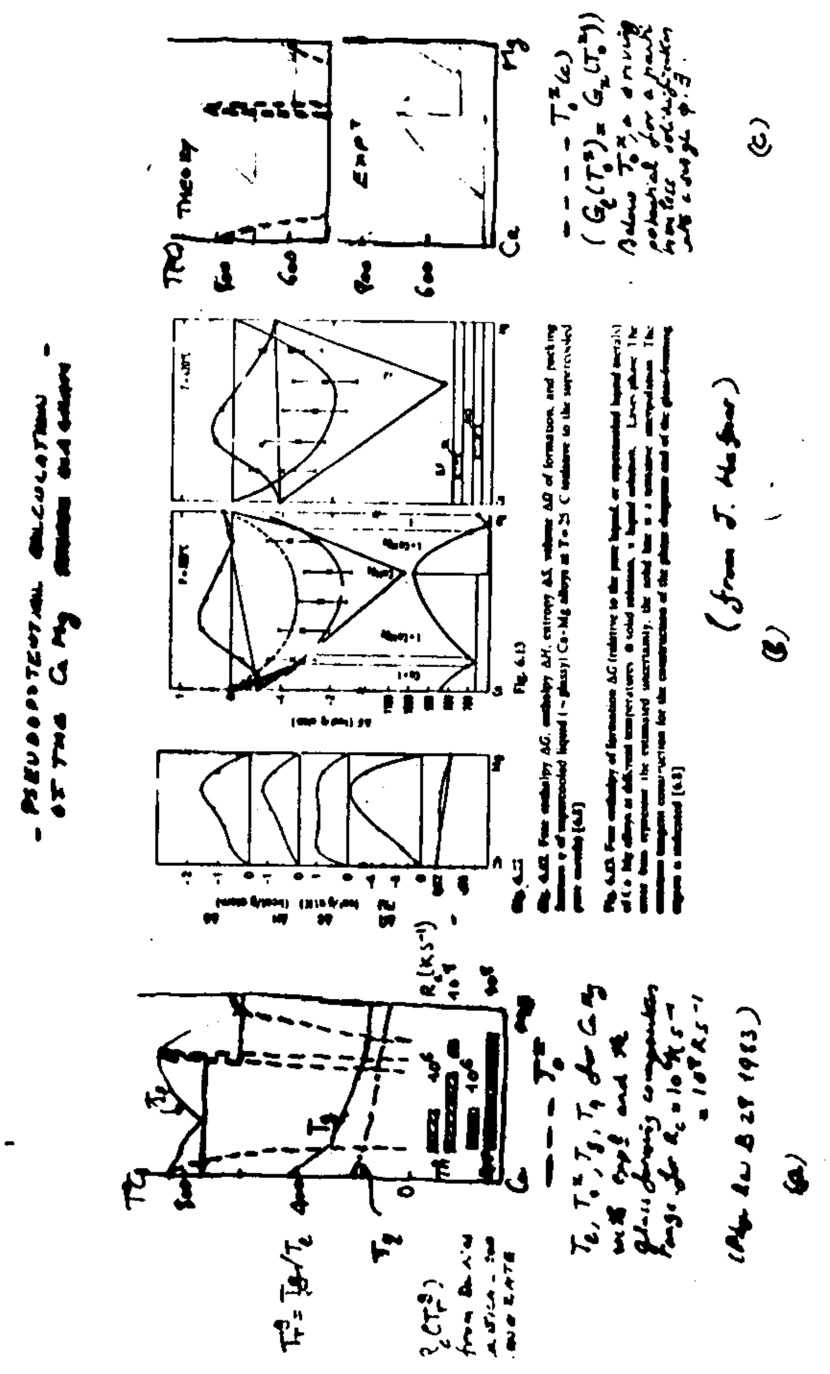

The phase diagram we use as a guide has been calculated from the pseudopotential theory using the Bogoliubov inequality to determine the free enthalpies of the liquid phase, the reference system being a hard sphere fluid. Some supplementary approximations have been done: (1) ΔS_{mix} for disordered Ga Mg alloys was assumed to be equal to the ideal one. (2) The entropy of formation of Ga rich intermetallic compounds was assigned to be zero and the entropy of formation of the homogeneous phase has been taken from experiment. Finally the energy difference between the solid and liquid phase has been slightly shifted to reproduce the exp. melting temperature of the pure metals. The comparison between exp. and th. phase diagrams is shown in fig (8). p. 58 But we now introduce some physical quantities which will allow to precise the domains of glass formation and discuss their values in relation with the previous phase diagram.

a) the thermodynamic temperature $T_0^m(c)$. (see fig (8))

T_0^m is defined by : $\phi_\beta(T_0^m, c) = \phi^m(T_0^m, c)$

Below this temperature a driving thermodynamic potential exists for a completely partitionless solidification into a single phase. In the regions limited by T_0^m, a composition invariant crystallization could occur preferentially and the LR is precluded.

b) the entropy crisis model T_0

The strong decrease of the fluidity η^{-1} (η is the viscosity) near T_g will lead to a strong decrease of S_{conf}. The temperature T_0 is defined by :

$$\phi_\beta(T_0) = S_\alpha(T_0)$$

The curves $T_0(c)$ define a lower bound of the glass transition temperature T_g. and T_g can be thought (Kauzmann) to tend to a T_0 for low cooling rate R.

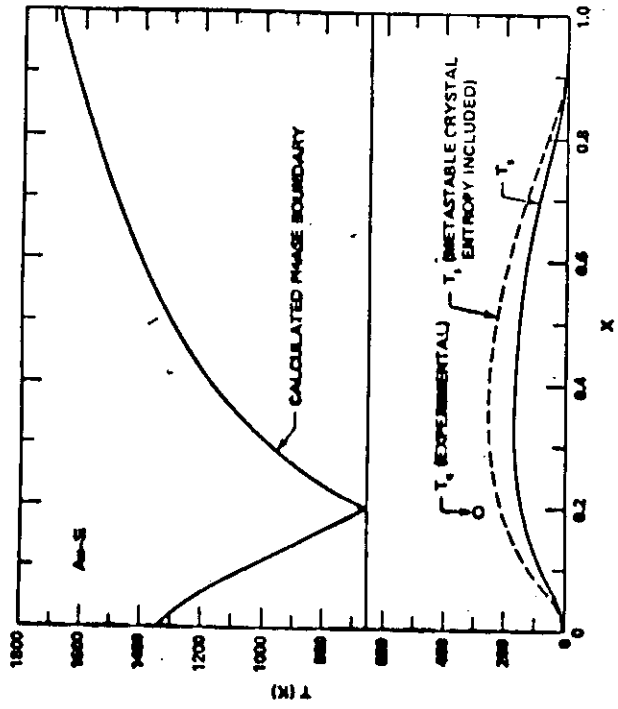

Fig. 5 The composition dependence for Al-Si of the temperature of vanishing liquid-solid entropy difference for (solid line) the phase separated solid and (dashed line) the intermediate metastable solid. The experimental glass transition temperature is shown by a point.

In the theoretical model for Ca-Mg system T_0 can be calculated ΔT_0's found to be rather independent of c (fig (a) and below).

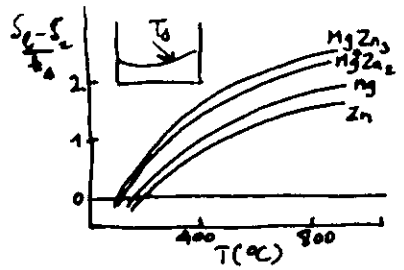

On the contrary, for solutions with strong chemical interactions, the strong negative entropy of the supercooled liquid (see Au-Si) leads to a maximum of T_0 (see fig). A large enthalpy of formation ($\Delta H_m < 0$) which implies a strong C.S.R.O. will thus favor large values of T_0 and can then be thought to imply an easy GFA.

b) <u>The free volume model and the temperature T_η</u>

A glassy state is thought to be an extension of the liquid state for which the viscosity becomes larger than $\eta = 10^{13}$ P.

In the free volume model η is related to the free volume by

$$\eta = \eta_0 \exp V/V_f$$

where V_f is the average free volume of the liquid. The maximum packing fraction of the normal metals and alloys is theoretically found to be $\pi \cdot \sqrt{2}/6$ so that $V_f = V - V_{cp}$ where V_{cp} is the atomic volume at random close packing. η_0 can be derived from a calculation of the viscosity near T_ℓ (via the self diffusion coefficient D)

The temperature T_η is such that $\eta(T_\eta) = 10^{13}$ P

T_η is related to T_g since both are related to the decrease of the free volume (see fig (a))

c) <u>glass forming composition ranges</u>.

Using the Davies curve, $R_c = R_c(T_{gr}, T_0)$ (see Amorphous metallic materials (Brotzen Love) 1980 p.107) we can determine the composition ranges of GF for given cooling rates R. For Ca-Mg the results are satisfactory. (see fig (b) p 18).

In these "weak interactions systems", the energetics of alloy phases is the determining factor for the glass formation whereas, in "strong interactions" systems, the variation of entropy with temperature related to the existence of SRO for decreasing T is an essential factor for the GFA.

<u>Conclusion</u>

The previous analysis allowed to define the relevant physical quantities which are related to the GFA. It showed that such quantities can be either calculated (T_0, T_0) or estimated T_g, compositions ranges for a given R). It suggests that there is no unique mechanism for the glass formation - even fast glasses quenched from the melt, have exhibited strange cases being identified. Similar analysis must be done for the prediction of amorphous alloy formation by ion beam mixing, solid state reactions ... in relation with thermodynamic data.